Seasonality in environment and population processes alters population spatial synchrony

Jonathan A. Walter[1,2]*
Daniel C. Reuman[3]
Kimberly R. Hall[4]
Herman H. Shugart[1]
Lauren G. Shoemaker[5]

1. Department of Environmental Sciences, University of Virginia, Charlottesville, Virginia 22904;
2. Center for Watershed Sciences, University of California, Davis, California 95616;
3. Department of Ecology and Evolutionary Biology & Center for Ecological Research, University of Kansas, Lawrence, Kansas 66047;
4. North America Science, The Nature Conservancy, Haslett, Michigan 48840;
5. Botany Department, University of Wyoming, Laramie, Wyoming 82071;

∗ Corresponding author; e-mail: jawalter@ucdavis.edu.

Manuscript elements: figure 1, figure 2, figure 3, figure 4, figure 5, table 1; figures 1, 2, 4, 5 are in color (and figures 1, 4, 5 are to print in color).

Keywords: Spatial synchrony, seasonality, breeding, overwintering, Moran effect.

Manuscript type: Article.

Prepared using the suggested LaTeX template for *Am. Nat.*

Abstract

Population spatial synchrony, the tendency for temporal population fluctuations to be correlated across locations, is common and important to metapopulation stability and persistence. One common cause of spatial synchrony, termed the Moran effect, occurs when populations respond to environmental fluctuations, such as weather, that are correlated over space. Although the degree of spatial synchrony in environmental fluctuations can differ between seasons and different population processes occur in different seasons, the impact on population spatial synchrony is uncertain because prior work has largely assumed that the spatial synchrony of environmental fluctuations and their effect on populations are consistent over annual sampling intervals. We used theoretical models to examine how seasonality in population processes and the spatial synchrony of environmental drivers affect population spatial synchrony using theoretical models. We found that population spatial synchrony can depend not only on the spatial synchrony of environmental drivers, but also on the degree to which environmental fluctuations are correlated across seasons, locally and across space. Moreover, measurements of synchrony from ”snapshot” population censuses may not accurately reflect synchrony during other parts of the year. Together, these results show that neglecting seasonality in environmental conditions and population processes is consequential for understanding population spatial synchrony and its driving mechanisms.

Introduction

Population spatial synchrony—the tendency for temporal fluctuations in the abundance of an organism to be correlated across locations—is a common phenomenon across ecological systems (Liebhold et al. 2004). Population synchrony results primarily from two key mechanisms: dispersal of individuals between locations (Abbott 2011; Bjørnstad et al. 1999; Koenig 1998) and demographic responses to environmental fluctuations that are themselves spatially correlated (i.e., Moran effects; Moran 1953). Spatial synchrony is notably important for rare and endangered species, as all else being equal more synchronous populations are expected to be more susceptible to extinction (Earn et al. 1998; Heino et al. 1997). Understanding factors that favor or disrupt synchrony is also highly relevant for anticipating and managing outbreaks of pests (Peltonen et al. 2002) and disease (Rohani et al. 1999; Viboud et al. 2006) and for the sustainability of yields of exploited organisms (Ong et al. 2021; Schindler et al. 2015). These applications have motivated a long history of study in both empirical and theoretical contexts.

Despite longstanding interest in population spatial synchrony, one notable knowledge gap is the role of seasonality in shaping patterns of spatial synchrony. By seasonality, we mean: (1) that different population processes (e.g., birth, migration, mortality) tend to be concentrated in different seasons, (2) that dominant environmental drivers of population dynamics may differ among seasons (Lima et al. 2002; Töpper et al. 2018), and (3) that seasons may differ in the degree of spatial correlation of environmental drivers (environmental synchrony). Seasonal separation of population processes can have profound impacts on population dynamics (Åström et al. 1996; Boyce et al. 1999; Kot and Schaffer 1984). As an example of dominant drivers differing among seasons, rainfall plays a key role in mediating aboveground plant competition and seed production during growing season months (Hallett et al. 2019), while temperature can play a key role in dormancy breaking and seed germination at the start of the growing season (Honda 2008). Analyses of environmental drivers show that temperature is generally more strongly spatially correlated than precipitation across spatial scales (Koenig 2002). Moreover, there are seasonal differences in patterns of spatial correlation of temperature and rainfall: in North America, both exhibit greater correlations extending over longer distances during winter than summer (Koenig and Liebhold 2016). Thus, there is empirical evidence that seasonality could impact spatial synchrony in three key ways; however, the consequences of these phemonena are unclear.

The empirical literature on population spatial synchrony offers clues that seasonality may have critical influences on spatial synchrony, even though few studies have addressed this directly. Across multiple species, birds have been observed to exhibit greater spatial synchrony during overwintering than breeding seasons (Koenig 1998), yet the reasons for this difference remain unclear. Furthermore, several studies have concluded that spatial synchrony is driven by environmental fluctuations during particular times of year. For example, Anderson et al. (2021) found that climate oscillations influencing winter weather were a primary driver of spatial synchrony in deer abundances in Wisconsin, USA. Fall, but not winter, precipitation was an apparent driver of spatial synchrony for the annual herb *Plantago erecta* (Walter et al. 2021). Synchronous winter temperatures drove synchrony in the phenology of British aphids (Sheppard et al. 2016). While examples such as these strongly suggest that we cannot fully understand synchrony without considering seasonality, the mechanisms underlying the role of seasonality in each example are unclear. The apparent influence of seasonality could relate to underlying ecology via the mechanisms described above. Independent of ecological mechanisms, however, some seasons could appear more important than others due to their proximity to sampling events.

Despite some empirical evidence for the importance of seasonality to spatial synchrony, a general understanding is unlikely to arise through empirical study alone. Long, multi-location time series suited to studying spatial synchrony are rare in proportion to the total number of ecological datasets, and records with regular observations across multiple seasons rarer still. Furthermore, disentangling pattern from process may be difficult in purely observational data (Abbott 2011; Kendall et al. 2000). In such cases where a lack of data hinders a robust general understanding, theory is valuable for assessing whether, and under what conditions, some phenomenon alters predictions about outcomes of interest. Such results can, in turn, guide future study design and sampling protocols, and aid in conservation and management. However to date, theoretical investigations of spatial synchrony have largely assumed simple functional forms of population dynamics and consistent environmental synchrony across time steps or sampling intervals (e.g., Engen and Sæther 2016; Heino et al. 1997; Moran 1953); it is unclear how simple but realistic violations of these assumptions alter expectations concerning population synchrony and its relationship to environmental drivers.

In this study we use theoretical models to examine how seasonality in population processes and in environmental drivers shapes population spatial synchrony. We first establish a general theoretical model and derive an analytical result showing that, when there is seasonality in population processes and environmental drivers, population spatial synchrony depends on details of population dynamics, the spatial synchrony of environmental drivers, and the degree to which environmental drivers are correlated across seasons in the same location and between locations. We then use simulations to show that a) our theory is robust to certain violations of simplifying assumptions; b) measurements of population synchrony can depend substantially on the timing of sampling relative to population processes; and c) both seasonality in population processes and seasonal differences in environmental drivers are important determinants of population spatial synchrony. We examine how seasonality alters classic predictions concerning the effects of environmental drivers (Moran effects) on synchrony. Our findings imply strongly that "cross-season" synchrony, i.e., correlations between environmental drivers in different seasons, in the same location and between different locations, shapes the spatial synchrony of populations; however, this phenomenon has received little attention.

Methods

This study considers population dynamics across locations (patches) in which there is a summer breeding season during which offspring are produced and individuals may perish, and an overwintering season during which individuals may perish only. In the interest of biological concreteness we use the terms "breeding" and "overwintering" appropriate for an animal study system, but we note that general insights from this model extend to other organisms including plants that reproduce during a particular season, and which then must survive until the next reproductive opportunity. Population dynamics in the breeding and overwintering seasons are subject to the influence of environmental drivers, which may be correlated between patches and seasons. For simplicity, and since synchrony is commonly measured in a pair-wise manner, we consider a two-patch model in which spatial scale is arbitrary; nonetheless, since the strength of spatial correlation in environmental drivers tends to decline with distance (Di Cecco and Gouhier 2018; Koenig 2002), one might imagine differing degrees of environmental synchrony as corresponding to different distances between patches. First, we develop an analytical solution showing how seasonality affects overall population synchrony under reasonable and common simplifying assumptions. Second, we use simulation to strengthen understanding of the underlying dynamics and to compare results to alternative models with more commonly considered assumptions.

Analytical Theory

We consider the model

$$N_i(t) = N_i(t-1)f\big(N_i(t-1), \epsilon_{B,i}(t)\big) \cdot s\big(N_i(t-1)f\big(N_i(t-1), \epsilon_{B,i}(t)\big), \epsilon_{W,i}(t)\big), \tag{1}$$

where $N_i(t)$ is population density in patch i at time t; the function $f(N, \epsilon_B)$ corresponds to breeding season population growth; and the function $s(B, \epsilon_W)$ is an overwintering survival rate. Each timestep t begins with breeding, followed by overwintering, and the model advances to the next timestep after overwintering. The population density following the breeding season is denoted B, which like N may be indexed by patch i and time t. The variables ϵ_B and ϵ_W represent environmental drivers during the breeding and overwintering seasons, respectively. In empirical settings, ϵ_B and ϵ_W might be thought of as the same environmental variable (e.g., temperature) measured in two different seasons, alternatively as distinct environmental drivers (e.g. temperature, precipitation) that are important at different times of year, or even multivariate combinations of environmental conditions in different seasons.

We consider the two-patch case of this model, and for simplicity ignore dispersal while deriving our analytical result. We assume $f > 0$ and $\partial f / \partial N < 0$, so that increasing pre-breeding density always reduces the per-capita population growth rate during the breeding season. We do not assume $f > 1$, so net loss during the breeding season may occur. We assume $\partial f / \partial \epsilon_B > 0$, so that higher values of the breeding-season environmental variable enhance per-capita breeding season population growth. We assume $0 < s < 1$, and $\partial s / \partial B < 0$, so that increasing post-breeding-season population density always decreases the overwintering survival rate. We assume $\partial s / \partial \epsilon_W > 0$, so that higher values of the winter environmental variable always enhance winter survival. We adopted the convention that larger values of environmental variables are always "good" for the population. This convention is arbitrary, but is adopted without loss of generality. For simplicity, we assume the four-dimensional random variables $(\epsilon_{B,i}(t), \epsilon_{B,j}(t), \epsilon_{W,i}(t), \epsilon_{W,j}(t))$ are independent and identically distributed (iid) across time (thus their t argument can usually be dropped); and that $(\epsilon_{B,i}, \epsilon_{W,i})$ and $(\epsilon_{B,j}, \epsilon_{W,j})$ are identically distributed and $(\epsilon_{B,i}, \epsilon_{W,j})$ and $(\epsilon_{B,j}, \epsilon_{W,i})$ are identically distributed. The first of these assumptions is an assumption of white-noise environmental conditions, which implies stationarity, and the second and third assumptions make our model spatially homogeneous.

Our main interest is to determine how spatial synchrony (the Pearson correlation between $N_i(t)$ and $N_j(t)$) depends on the parameters of this model, and thus on seasonality in population dynamics and in environmental drivers. Moran (1953) stated that for fluctuating populations $N_i(t)$ governed by identical linear dynamics subject to environmental perturbations (i.e., environmental noise or stochasticity, $\epsilon_i(t)$, where $N_i(t) = aN_i(t-1) + \epsilon_i(t)$), population spatial synchrony is equal to the degree of correlation in environmental perturbations; that is, considering two patches $i \neq j$: $\mathrm{cor}(N_i(t), N_j(t)) = \mathrm{cor}(\epsilon_i(t), \epsilon_j(t))$. We build from this observation, known as the "Moran theorem," to investigate how seasonality influences spatial synchrony.

We begin by linearizing our model and then analyze the linearized version. We assume that the one-patch, deterministic version of our model has a positive stable equilibrium N^* and linearize it at the equilibrium. Defining

$$g(N, \epsilon_B, \epsilon_W) = Nf[N, \epsilon_B]s[Nf[N, \epsilon_B], \epsilon_W], \tag{2}$$

$$n_i(t) = N_i(t) - N^*, \tag{3}$$

$$e_{B,i}(t) = \epsilon_{B,i}(t) - \bar{\epsilon}_B, \tag{4}$$

$$e_{W,i}(t) = \epsilon_{W,i}(t) - \bar{\epsilon}_W, \tag{5}$$

linearizing gives

$$n_i(t) \approx P_A n_i(t-1) + P_B e_{B,i}(t) + P_W e_{W,i}(t) \tag{6}$$

where

$$P_A = \left[\frac{\partial g}{\partial N} \right|_{(N^*, \bar{\epsilon}_B, \bar{\epsilon}_W)} \tag{7}$$

$$P_B = \left[\frac{\partial g}{\partial \epsilon_B} \right|_{(N^*, \bar{\epsilon}_B, \bar{\epsilon}_W)} \tag{8}$$

$$P_W = \left[\frac{\partial g}{\partial \epsilon_W} \right|_{(N^*, \bar{\epsilon}_B, \bar{\epsilon}_W)} . \tag{9}$$

This is an autoregressive moving average-like model, which can be subjected to a wide range of mathematical analyses.

To determine the spatial synchrony of two locations i, j whose dynamics follow eq. 6, we compute the Pearson correlation cor(n_i, n_j) by computing the covariance cov(n_i, n_j) and the variances var(n_i) and var(n_j). Making use of the above assumptions about the environmental drivers ϵ_B and ϵ_W, we determine the spatial synchrony in population abundances cor(N_i,N_j) to be:

$$\mathrm{cor}(N_i, N_j) \approx \frac{P_B^2 \,\mathrm{cov}(\epsilon_{B,i}, \epsilon_{B,j}) + P_W^2 \,\mathrm{cov}(\epsilon_{W,i}, \epsilon_{W,j}) + 2P_B P_W \,\mathrm{cov}(\epsilon_{B,i}, \epsilon_{W,j})}{P_B^2 \,\mathrm{var}(\epsilon_{B,i}) + P_W^2 \,\mathrm{var}(\epsilon_{W,i}) + 2P_B P_W \,\mathrm{cov}(\epsilon_{B,i}, \epsilon_{W,i})}. \tag{10}$$

See Online Appendix A for added detail about this derivation.

The first two terms in the numerator relate to traditional measures of spatial synchrony of environmental variables, but there are also contributions from “cross-season” synchrony, both between and within locations (in the numerator and denominator, respectively). Hence, we predict that the spatial synchrony of populations influenced by season-specific environmental drivers is sensitive not only to the spatial synchrony (spatial covariances) in each environmental driver, but also to the degree of covariance in environmental drivers between seasons in the same location, and the degree to which environmental drivers in different seasons co-vary across different locations. We conducted a simple exploration of cross-season synchrony using summertime and wintertime temperatures and precipitation across the conterminous United States and found that strength of such correlations varies widely with substantial positive and negative values possible (i.e. Pearson correlations range from ≈ -0.5 to 0.5) (Online Appendix B). We concluded from this exploration that substantial cross-season synchrony in environmental conditions is possible, but more detailed exploration is needed to resolve its spatiotemporal structures; for this study we consider a range of influences from no to moderate degrees of cross-season synchrony.

Using the analysis above, we also predict that spatial synchrony depends on terms related to the quantitative effects of environmental variation on population growth (P_B^2, P_W^2, $P_B P_W$). These quantities are affected by $f(N, \epsilon_B)$ and $s(B, \epsilon_W)$, and hence are related to details of population growth and survival. We found a primary manifestation of this dependence to be that certain relationships between environmental synchrony and population synchrony depend on whether population growth is undercompensatory or overcompensatory.

Defining a Specific Model

To illustrate the sensitivity of population spatial synchrony to the elements of (eq. 10), we examine a specific model that is a straightforward case of (eq. 1). We define

$$f(N, \epsilon_B) = \exp(f_0) \exp(-N/k_B) \exp(\epsilon_B) \tag{11}$$

and

$$s(B, \epsilon_W) = \exp(s_0) \exp(-B/k_W) \exp(\epsilon_W), \tag{12}$$

where B is the population size after the breeding season. Choosing a particular model allows computation of P_A and P_W (eq. 8-9), key variables in eq. 10, based on parameters in a specific population dynamic model. For use in quantitative explorations of parameter sensitivity, we here introduce the "relative survival rate" $\hat{s}_0$, where $s_0 = \hat{s}_0 f_0$. Doing so ensures we analyze scenarios of biologically meaningful densities and is consistent with the analytical solution above such that $s_0 \leq f_0$. Most importantly, temporal population dynamics are determined by the interplay of population growth and survival rates. Analyzing $\hat{s}_0$ allows us to define areas of parameter space where dynamics are overcompensatory versus undercompensatory. Consistent with assumptions of Moran (1953), we assume that the population dynamic parameters f_0, k_B, s_0, and k_W are uniform across locations. We also begin by assuming the environmental drivers ϵ_B and ϵ_W are zero-mean normally distributed random variables and independent through time, and that there may be correlations between $\epsilon_{B,i}$ and $\epsilon_{B,j}$; $\epsilon_{W,i}$ and $\epsilon_{W,j}$; $\epsilon_{B,i}$ and $\epsilon_{W,i}$; and $\epsilon_{B,i}$ and $\epsilon_{W,j}$. Throughout, we consider the case in which cross-season environmental synchrony is the same within and between locations, i.e., $\text{cor}(\epsilon_{B,i}, \epsilon_{W,i}) = \text{cor}(\epsilon_{B,j}, \epsilon_{W,j}) = \text{cor}(\epsilon_{B,j}, \epsilon_{W,i}) = \text{cor}(\epsilon_{B,i}, \epsilon_{W,j})$, but that need not be the case. Note that because we consider this particular case our notation omits the patch subscripts i, j when referencing correlations among environmental drivers in different seasons. We also assume throughout that environmental drivers are equally temporally variable across seasons and locations ($\sigma_B = \sigma_W$), but that the variances of environmental drivers can change between model scenarios; this assumption helps ensure that differences in population spatial synchrony result only from separation of population processes into distinct seasons or from differences between seasons in the synchrony of environmental drivers. Although our solution (eq. 10) is expressed in terms of covariances and variances, we generally express model inputs and outputs in terms of correlations and standard deviations because those are more common in empirical studies of spatial synchrony and population dynamics, generally.

We first examine synchrony dynamics of our analytical solution (eq. 10) as applied to model eqs. 11 and 12. To show general trends in spatial synchrony, we systematically vary both the breeding season (ϵ_B) and overwintering (ϵ_W) environmental correlations between locations, the relationship between growth rate (f_0) and the relative survival rate ($\hat{s}_0$), and finally the degree of cross season synchrony, $\text{cor}(\epsilon_B, \epsilon_W)$. We then show how patterns of parameter dependence depend on over- versus undercompensatory population growth, calculating spatial synchrony across a range of growth rates (f_0) from 0.3 to 2.45 and relative survival rates ($\hat{s}_0$) from -0.9 to 0. The under- and overcompensatory regimes were determined from the deterministic skeleton of our model.

Simulations

We next conducted a simulation study that allowed us to relax some assumptions that we made above for analytical convenience. Earlier, for analytical tractability, we assumed a form of overwintering-season dynamics in which population increases during the overwintering season were possible. In simulation, we modified eq. 12 so that overwintering-season population increases were not possible:

$$s(B, \epsilon_W) = \min\big(\exp(s_0)\exp(-B/k_W)\exp(\epsilon_W),\ 1\big). \tag{13}$$

We relaxed the assumption of no dispersal by specifying a fraction d of each population i, j to be exchanged with the other. We also tested the sensitivity of our results to interannual correlation in environmental conditions; while we focus in the main text on the case of white noise environmental drivers (interannual lag-1 autocorrelation = 0), we also conducted simulations in which environmental drivers had first-order autoregressive [AR(1)] structure with AR(1) coefficients of -0.5, -0.2, 0.2, and 0.5 (Online Appendix C). Our simulations work directly with nonlinear equations, not linearizations thereof.

We compared predictions of population spatial synchrony, $\mathrm{cor}(N_1(t), N_2(t))$, from our analytically obtained solution to population spatial synchrony computed from simulations to evaluate consistency between our analytical solution, which is an approximation due to the assumptions facilitating analytical tractability, and simulations that allowed relaxing some of our strictest assumptions. We show a selection of results in Online Appendix Fig. S1 across multiple regions of parameter space, and found strong agreement between our analytical and simulation-based estimates of population spatial synchrony.

In addition, to better understand how the combination of seasonality in population processes and multiple environmental drivers contributes to our results, we compared results for our main model with results from two alternate models that make different assumptions about seasonality in population processes and environmental drivers.

For our main simulation model, we use the special case of eq. 1 we defined above (eq. 11, 13). One alternate model, which we denote the "no overwintering" model, examines the case in which there are two environmental drivers acting on the population, but there is no separation of population dynamics into distinct seasons. In this case, $f(N, \epsilon_B) = \exp(f_0)\exp(-N/k_B)\exp(\epsilon_B)\exp(\epsilon_W)$, and $s(B, \epsilon_W)$ is disregarded. We retain the notation ϵ_B and ϵ_W because the consistency aids comparison across model formulations, but under this formulation the ϵ are not regarded as happening in any particular season. This formulation is similar to, in eq. 12, setting $s_0 = 0$ and $k_W = \infty$, and hence eq. 10 could provide an approximate solution.

The other alternate model considered here, which we denote the "same environment" model, examines the case in which population processes are separated into two distinct seasons, but the environmental driver in each season is identical, i.e., $\epsilon_B = \epsilon_W$. This version is equivalent to $\text{cor}(\epsilon_B, \epsilon_W) = 1$, and again eq. 10 could provide an approximate solution.

We used a simulation experiment to test the sensitivity of spatial synchrony, $\text{cor}(N_i(t), N_j(t))$, to parameter variability, and how this sensitivity differed between our main and alternate models. Latin hypercube sampling (Stein 1987) was used to efficiently survey the space of parameter combinations in 300 replicates, using distributions of individual parameters shown in Table 1. The chosen ranges for f_0, k_B, $\hat{s}_0$, and k_W produce undercompensatory to overcompensatory population growth, but not period-doubling or chaotic oscillations. The density dependence parameter k_W was specified as a fraction of k_B, corresponding to an assumption that $k_W <= k_B$. Simulations were run for 10,000 time steps, with the first 1,000 time steps discarded to remove effects of initial conditions. We then used multiple linear regression to examine how spatial synchrony in population abundances $N_i(t)$ depended on each parameter. Prior to regression analysis, all main effect predictors were scaled to have mean = 0 and standard deviation = 1 so that regression coefficients can be interpreted as relative effect sizes. In addition to comparing relative effect sizes of parameters for our main simulation model, we also compare results for our main model with those from the "same environment" and "no overwintering" alternate model formulations described above, facilitating comparisons between the main model and two more common assumptions for seasonality.

Next, to focus on impacts of seasonal differences in the synchrony of environmental drivers on population spatial synchrony, we varied breeding season environmental synchrony ($\mathrm{cor}(\epsilon_{B,i}, \epsilon_{B,j})$) and overwintering season environmental synchrony ($\mathrm{cor}(\epsilon_{W,i}, \epsilon_{W,j})$) independently while holding other parameters constant. Both $\mathrm{cor}(\epsilon_{B,i}, \epsilon_{B,j})$ and $\mathrm{cor}(\epsilon_{W,i}, \epsilon_{W,j})$ took values 0, 0.05, 0.1, ... 1, and 75 replicate simulations were run for all combinations of $\mathrm{cor}(\epsilon_{B,i}, \epsilon_{B,j})$ and $\mathrm{cor}(\epsilon_{W,i}, \epsilon_{W,j})$. Each simulation was run for 2,000 time steps, with the first 1,000 discarded to remove effects of initial conditions. Cross-season synchrony ($\mathrm{cor}(\epsilon_B, \epsilon_W)$) took the values -0.2, 0, and 0.2; see Online Appendix C for results when $\mathrm{cor}(\epsilon_B, \epsilon_W) = -0.2, 0$. Because of the differences between under- and overcompensatory dynamics, we show results from parameterizations that create under- and overcompensatory dynamics by manipulating f_0; $f_0 = 1$ (undercompensatory) or $f_0 = 2$ (overcompensatory). Other parameters were held constant at $k_B = 100$, $\hat{s}_0 = -0.1$, $k_W = 80$, $\mathrm{cor}(\epsilon_B, \epsilon_W) = 0.2$, and $\mathrm{sd}(\epsilon) = 0.1$.

We used these simulations to make two primary comparisons. The first examines the importance of assumptions about seasonality in population processes and environmental drivers by comparing results from our main simulation with those from the "same environment" and "no overwintering" alternate model formulations described above. The second examines the importance of timing of sampling. Here, we compared spatial synchrony entering the new breeding season (i.e., $\mathrm{cor}(N_i(t), N_j(t))$) to spatial synchrony between the breeding and overwintering seasons (i.e., $\mathrm{cor}(B_i(t), B_j(t))$). Parallel results with $\mathrm{cor}(\epsilon_B, \epsilon_W) = 0$ and $\mathrm{cor}(\epsilon_B, \epsilon_W) = -0.2$ are reported in Figures S.2-S.5.

Code reproducing this study is available on Zenodo at https://doi.org/10.5281/zenodo.7881163.

Simulations and analyses were implemented in R version 4.2.1 (R Core Team 2021).

Results

Our analytical results (eq. 10) predict that population spatial synchrony depends on details of population dynamics [$f(N, \epsilon_B)$ and $s(B, \epsilon_W)$], the spatial synchrony of environmental drivers [$\mathrm{cor}(\epsilon_{B,i}, \epsilon_{B,j})$ and $\mathrm{cor}(\epsilon_{W,i}, \epsilon_{W,j})$], and covariance between environmental drivers for different seasons, both in the same location [$\mathrm{cor}(\epsilon_{B,i}, \epsilon_{W,i})$] and between locations [$\mathrm{cor}(\epsilon_{B,i}, \epsilon_{W,j})$]. The nature of these dependencies for our chosen model (eqs. 11, 12) are illustrated in Figure 1. Population spatial synchrony changes with environmental synchrony as a weighted average of environmental synchrony during the breeding and overwintering seasons, here more strongly influenced by the overwintering season. Further, population spatial synchrony can be negative despite positive correlations in environmental drivers, as exemplified with this model parameterization (Figure 1a). Population synchrony also depends nonlinearly on cross-season synchrony (Figure 1b), with the direction of the relationship (positive or negative) depending on whether population dynamics are undercompensatory (black, green) or overcompensatory (blue, red). Note that we here considered the case where $\mathrm{cor}(\epsilon_{B,i}, \epsilon_{W,i}) = \mathrm{cor}(\epsilon_{B,i}, \epsilon_{W,j})$ but this need not be the case.

With seasonality, population synchrony also depends nonlinearly on the population growth and survival rates (Figure 1c). However, the direction of these effects is contingent on whether population dynamics are in the undercompensatory or overcompensatory regime, and on whether $\mathrm{cor}(\epsilon_{B,i}, \epsilon_{B,j}) > \mathrm{cor}(\epsilon_{W,i}, \epsilon_{W,j})$ (Figure 2). Population synchrony was highest when relative survival and growth rates were either both low or high. Interestingly, the shape of the nonlinearities between f_0 and $\hat{s}_0$ are consistent, though their magnitude varies with the strength of $\mathrm{cor}(\epsilon_{B,i}, \epsilon_{B,j})$ and $\mathrm{cor}(\epsilon_{W,i}, \epsilon_{W,j})$ and the directionality depends on if $\mathrm{cor}(\epsilon_{B,i}, \epsilon_{B,j}) > \mathrm{cor}(\epsilon_{W,i}, \epsilon_{W,j})$ (Figure 2).

Our simulation results agreed with our analytical results, demonstrating their robustness to certain violations of the assumptions enabling analytical tractability of our model (Figure S.1). For our main model, sensitivity of population synchrony to variation in model parameters was generally consistent with predictions from analytical theory (Figure 3). Separating cases when the population dynamic regime was under- or overcompensatory and with $\mathrm{cor}(\epsilon_{B,i}, \epsilon_{B,j})$ greater or less than $\mathrm{cor}(\epsilon_{W,i}, \epsilon_{W,j})$ addressed major sources of nonlinearity and allowed remaining parameter dependencies to be reasonably approximated by linear effects. Consistently across these cases, overwintering season environmental synchrony [$\mathrm{cor}(\epsilon_{W,i}, \epsilon_{W,j})$] and cross-season synchrony [$\mathrm{cor}(\epsilon_B, \epsilon_W)$] had large effects, although the direction of the effect of $\mathrm{cor}(\epsilon_B, \epsilon_W)$ depends on population dynamic regime. When $\mathrm{cor}(\epsilon_{B,i}, \epsilon_{B,j}) > \mathrm{cor}(\epsilon_{W,i}, \epsilon_{W,j})$, the population growth rate f_0 and relative survival rate s_0 had large effects whose direction depended on population dynamic regime (Figure 3). Simulation also allowed us to address the effects of dispersal: consistent with canonical expectations, increasing the dispersal rate tended to increase spatial synchrony (Figure 3), and the effects of seasonality remained qualitatively similar (Figures S.8, S.9). Similarly, the effects of interannual autocorrelation in environmental drivers accorded with expectations from prior work (Heino 1998). Interannual autocorrelation increased spatial synchrony, but did not qualitatively alter the effects of seasonality (Figures S.10, S.11).

Comparison of our main model to two alternate models making different assumptions about seasonality in population processes and environmental drivers demonstrates how both influence the dependence of population spatial synchrony on environmental synchrony and other model parameters. Removing the separation of population processes into breeding and overwintering seasons tended to increase the importance of f_0, K_B, breeding season environmental synchrony, and cross-season environmental synchrony (Figure 3). Having the breeding and overwintering seasons affected by the same environment tended to increase the importance of environmental synchrony and altered the dependence of population synchrony on population dynamic parameters such as f_0 and s_0 in ways that depended on population dynamic regime (Figure 3). Seasonality in both the environment and population processes yields “weighting factors” for the effects of season on population synchrony (Figure 4a,d). In comparison, under the “no overwintering” and “same environment” alternate models, population synchrony increased as a linear function of environmental synchrony, with equal weighting of the breeding and overwintering environments in the “no overwintering” model (Figure 4b,e). In the “same environment” model, population synchrony depends directly on environmental synchrony, following the Moran theorem (Figure 4c,f).

Importantly for empirical investigations of synchrony, differences in when a population is censused could lead to marked differences in measures of population synchrony and its dependence on the synchrony of environmental drivers. For example, using the same model, we observe striking variation in $\mathrm{cor}(N_t)$ versus $\mathrm{cor}(B_t)$, leading to differences in measured population synchrony up to ± 0.3 (Figure 5). Spatial synchrony of breeding populations depends more heavily on the breeding season environment (Figure 5b,e), while spatial synchrony of the overwintering populations depended on both seasonal environments, with the winter environment weighted more heavily (Figure 5a,d).

Discussion

For many organisms, from microbes that bet-hedge through stressful environmental conditions via dormancy (Jones and Lennon 2010; Wisnoski and Lennon 2021) to plants with distinct periods of growth and seed production (Harper et al. 1977), to highly migratory mammals with winter and summer ranges (Sawyer et al. 2016), different life-history stages and demographic processes are concentrated during distinct seasons—and for migratory species in distinct locales. Various population processes may be linked to different environmental cues, such as temperature, precipitation, or food availability, suggesting that environmental cues during a specific season may be especially important for a given demographic process (Aikens et al. 2017; Hallett et al. 2019). Different seasons and locations also exhibit different spatiotemporal patterns of environmental variation (Di Cecco and Gouhier 2018; Koenig 2002), implying that seasonality could have substantial consequences for spatial population synchrony. Using theoretical models, here we mechanistically showed that incorporating seasonality in population processes and environmental drivers consistently alters the relationship between environmental drivers and population spatial synchrony. For example, seasonality can cause population synchrony to be greater than environmental synchrony in the absence of dispersal (Figure 4a), contradicting conventional expectations, and representing a case of interacting Moran effects (Castorani et al. 2022; Sheppard et al. 2019). Alternatively, seasonality can lead to negative population spatial synchrony despite positive Moran effects (Figure 4d). More generally, the interplay of environmental drivers and population growth, specifically the degree of over- or undercompensatory dynamics, yields strong impacts of seasonality on population synchrony (Figure 2). Finally, we showed that empirical measurements of synchrony likely depend on the season of sampling (Figure 5), identifying a new challenge in connecting patterns of population spatial synchrony to mechanism and suggesting that consistency in the season of sampling is critical for empirically testing patterns of synchrony. The ubiquity of seasonal effects on ecological populations, and their importance for population synchrony as shown here, emphasizes that theoretical and empirical investigations should consider the impact of “cross-season” synchrony.

The Moran theorem predicts, under certain assumptions, that population spatial synchrony will equal the spatial correlation in an environmental driver (Moran 1953). Intuitively, one might expect that, in a case with multiple environmental drivers, population spatial synchrony should equal the average synchrony of the environmental drivers, consistent with what we observed in the “no overwintering” model (Figure 4). However, we showed that when population processes were separated into distinct seasons, population synchrony was instead a weighted average of the synchrony of the environments in the distinct seasons. In the cases considered in this study, the weights reflect differences in population processes across the seasons, but our theory (eq. 10) predicts that differences in variance between the environmental driver—or, equivalently, differences in sensitivity of population dynamics to the environmental drivers—could also weight the effects of distinct seasons differently. More broadly, our results demonstrate how a simple addition of biological realism to a theoretical model can lead to marked changes in population spatial synchrony and its relationship to environmental drivers. Although some aspects of our results are intuitive, others—such as the dependence of the population synchrony-environmental synchrony relationship on population dynamic regime and the importance of cross-season synchrony—were more surprising. Consequently, we assert that further efforts to increase the biological realism of population models in studies of spatial synchrony are likely important to improved understanding of synchrony itself and closely related phenomena like metapopulation stability and persistence.

A key finding of our study is the importance of what we termed "cross-season" or "cross-variable" synchrony, i.e., correlations in environmental drivers between seasons, both in the same location and between different locations. A primary way that cross-season synchrony affected population synchrony in our results was to increase or decrease population synchrony when spatial synchrony in the breeding and overwintering environments was low, including creating cases where population spatial synchrony was *greater than* the synchrony of either environmental driver. Investigations of spatial synchrony have largely assumed that population spatial synchrony would be less than that of environmental conditions (Liebhold et al. 2004; Peltonen et al. 2002), and indeed our results are impossible under the assumptions of the classic Moran theorem. Further, we conducted a preliminary empirical investigation of cross-season synchrony in precipitation and air temperatures from which we concluded that weak to moderately strong positive and negative correlations between environmental conditions in different seasons were common (Online Appendix B), suggesting empirical patterns under which our theoretical results may be corroborated empirically. Future work should investigate the spatiotemporal structures of cross-season synchrony; for example, does it tend to decline with distance, and is it more prevalent in particular regions? Is it changing through time as a possible consequence of climate change?

Our theoretical findings have multiple implications for empirical studies of spatial synchrony. In particular, we found that measures of population synchrony depend strongly on the season of sampling (Figures 5). Differences in spatial synchrony measured from the Breeding Bird Survey and Christmas Bird Count (occurring in spring versus winter months) have presented an interesting conundrum (Koenig 1998). While multiple biological and methodological mechanisms (e.g. sampling protocol differences) may be at play, we posited that seasonality could explain differences in the spatial synchrony of bird populations during breeding and overwintering. This hypothesis was one of the primary motivations for this study, and our theoretical results offer one plausible explanation for this empirical phenomenon.

Many empirical synchrony studies have found season-specific drivers of population synchrony (e.g. Anderson et al. 2021; Sheppard et al. 2016; Walter et al. 2021). Here again, our theoretical results offer plausible explanations: we found that when population processes exhibited distinct seasonality, environmental conditions during one season had a greater effect on population synchrony (Figures 3, 4). Moreover, many studies attributing specific climatological drivers of spatial synchrony are of univoltine or multivoltine insect species (Haynes et al. 2013; Liebhold et al. 2004; Sheppard et al. 2016; Walter et al. 2020) that tend also to have short seasons of physiological activity separated by long periods of inactivity (e.g., overwintering eggs) during which individuals may be less sensitive to environmental variation (but see Sinclair 1999; Sinclair et al. 2013). By contrast, spatial synchrony seems less extensively studied in longer-lived taxa such as birds, mammals, and fish, and with fewer studies that conclusively attribute climatological drivers to population spatial synchrony (but see Anderson et al. 2021; Grenfell et al. 1998; Post and Forchhammer 2002). These longer-lived taxonomic groups are often physiologically active year-round and exhibit the sort of seasonal cycles in population processes that motivated this study. Thus, we speculate that seasonality has already played a role in the spatial synchrony literature by shaping for which organisms synchrony can be most reliably quantified and mechanisms attributed, given the available data and current methods. Better awareness of the potential influence of seasonality in the dynamics of longer-lived species could improve empirical attribution of mechanisms of synchrony by matching sampling periods to hypothesized drivers and considering how environmental drivers act on population processes such as fecundity, carrying capacity, or environmentally driven mortality events. For example, a new empirical approach to examining the impact of seasonality on synchrony is demonstrated in Nicolau et al. (2022), showing strong seasonal dependence of synchrony in vole populations, with winter weather a primary driver.

With ongoing climate change, the effect of seasonality on synchrony may be heightened. The temporal autocorrelation of environmental drivers has increased historically (Dillon et al. 2016; Koenig and Liebhold 2016) and is expected to increase further under climate change (Di Cecco and Gouhier 2018; Wang et al. 2015). A future increase in spatial autocorrelation is predicted given projections under current "business as usual" carbon emission scenarios (Di Cecco and Gouhier 2018). However, these changes in spatial synchrony of environmental drivers are expected to be both seasonally and geographically variable (Di Cecco and Gouhier 2018; Portmann et al. 2009). Increased differences between seasons given climate change may exacerbate both the patterns we identify here and the dependency of population synchrony on seasonal patterns. These large-scale climate drivers have already been shown to synchronize populations, even across large geographic distances (Post and Forchhammer 2002; Sheppard et al. 2016), with climate change effects on synchrony already documented (Post and Forchhammer 2004). If the synchrony of environmental drivers continues to change across seasons, our modeling results here suggest that we should expect impacts on population synchrony.

Conclusion

Seasonality in population processes and environmental drivers can alter expected patterns of population synchrony and variability. The present lack of recognition that seasonality shapes spatial synchrony and related population outcomes likely hinders fundamental understandings of synchrony, our ability to detect drivers empirically, and applications to conservation and natural resource management. Theoretical studies of spatial synchrony have predominantly adopted very simple models, including low-order autoregressive models (e.g., Moran 1953; Walter et al. 2017) and simple nonlinear models such as the Ricker equation (e.g., Heino et al. 1997), which trade off biological detail for tractability. Seasonality is just one of multiple ways that real populations can be dissimilar from the models predominating theory on spatial synchrony and informing empirical studies. We call for theoretical research on spatial synchrony to explore spatiotemporal patterns in cross-season synchrony and to incorporate distinct life-history periods in future modeling efforts, broadly addressing a range of ecologically realistic processes and grounding empirical observations.

Acknowledgments

This work was supported by a NatureNet Science Fellowship to JAW from The Nature Conservancy and The University of Virginia. LGS was supported by NSF 2033292 and 2019528.

Statement of Authorship

JAW, KRH, and HHS conceived the study. JAW, DCR, and LGS developed the theory. JAW and LGS drafted the manuscript. All authors contributed to manuscript revisions.

Data and Code Availability

Data and code are available at jonathan-walter. (2023). jonathan-walter/synchrony-seasonality-ms: Minor updates pre-publication (v1.0.1). Zenodo. https://doi.org/10.5281/zenodo.7881163

Literature Cited

Abbott, K. C. 2011. A dispersal-induced paradox: synchrony and stability in stochastic metapopulations. Ecology letters 14:1158–1169.

Aikens, E. O., M. J. Kauffman, J. A. Merkle, S. P. Dwinnell, G. L. Fralick, and K. L. Monteith. 2017. The greenscape shapes surfing of resource waves in a large migratory herbivore. Ecology Letters 20:741–750.

Anderson, T. L., L. W. Sheppard, J. A. Walter, R. E. Rolley, and D. C. Reuman. 2021. Synchronous effects produce cycles in deer populations and deer-vehicle collisions. Ecology Letters 24:337–347.

Åström, M., P. Lundberg, and S. Lundberg. 1996. Population dynamics with sequential density-dependencies. Oikos pages 174–181.

Bjørnstad, O. N., R. A. Ims, and X. Lambin. 1999. Spatial population dynamics: analyzing patterns and processes of population synchrony. Trends in Ecology & Evolution 14:427–432.

Boyce, M. S., A. Sinclair, and G. C. White. 1999. Seasonal compensation of predation and harvesting. Oikos pages 419–426.

Castorani, M. C., T. W. Bell, J. A. Walter, D. C. Reuman, K. C. Cavanaugh, and L. W. Sheppard. 2022. Disturbance and nutrients synchronise kelp forests across scales through interacting moran effects. Ecology letters 25:1854–1868.

Di Cecco, G. J., and T. C. Gouhier. 2018. Increased spatial and temporal autocorrelation of temperature under climate change. Scientific reports 8:1–9.

Dillon, M. E., H. A. Woods, G. Wang, S. B. Fey, D. A. Vasseur, R. S. Telemeco, K. Marshall, and S. Pincebourde. 2016. Life in the frequency domain: the biological impacts of changes in climate variability at multiple time scales. Integrative and comparative biology 56:14–30.

Earn, D. J., P. Rohani, and B. T. Grenfell. 1998. Persistence, chaos and synchrony in ecology and epidemiology. Proceedings of the Royal Society of London. Series B: Biological Sciences 265:7–10.

Engen, S., and B.-E. Sæther. 2016. Spatial synchrony in population dynamics: the effects of demographic stochasticity and density regulation with a spatial scale. Mathematical biosciences 274:17–24.

Grenfell, B., K. Wilson, B. Finkenstädt, T. Coulson, S. Murray, S. Albon, J. Pemberton, T. Clutton-

Brock, and M. Crawley. 1998. Noise and determinism in synchronized sheep dynamics. Nature 394:674–677.

Hallett, L. M., L. G. Shoemaker, C. T. White, and K. N. Suding. 2019. Rainfall variability maintains grass-forb species coexistence. Ecology Letters 22:1658–1667.

Harper, J. L., et al. 1977. Population biology of plants. Population biology of plants. .

Haynes, K. J., O. N. Bjørnstad, A. J. Allstadt, and A. M. Liebhold. 2013. Geographical variation in the spatial synchrony of a forest-defoliating insect: isolation of environmental and spatial drivers. Proceedings of the Royal Society B: Biological Sciences 280:20122373.

Heino, M. 1998. Noise colour, synchrony and extinctions in spatially structured populations. Oikos pages 368–375.

Heino, M., V. Kaitala, E. Ranta, and J. Lindström. 1997. Synchronous dynamics and rates of extinction in spatially structured populations. Proceedings of the Royal Society of London. Series B: Biological Sciences 264:481–486.

Honda, Y. 2008. Ecological correlations between the persistence of the soil seed bank and several plant traits, including seed dormancy. Plant Ecology 196:301–309.

Jones, S. E., and J. T. Lennon. 2010. Dormancy contributes to the maintenance of microbial diversity. Proceedings of the National Academy of Sciences 107:5881–5886.

Kendall, B. E., O. N. Bjørnstad, J. Bascompte, T. H. Keitt, and W. F. Fagan. 2000. Dispersal, environmental correlation, and spatial synchrony in population dynamics. The American Naturalist 155:628–636.

Koenig, W. D. 1998. Spatial autocorrelation in california land birds. Conservation Biology 12:612–620.

———. 2002. Global patterns of environmental synchrony and the moran effect. Ecography 25:283–288.

Koenig, W. D., and A. M. Liebhold. 2016. Temporally increasing spatial synchrony of north american temperature and bird populations. Nature Climate Change 6:614–617.

Kot, M., and W. Schaffer. 1984. The effects of seasonality on discrete models of population growth. Theoretical Population Biology 26:340–360.

Liebhold, A., W. D. Koenig, and O. N. Bjørnstad. 2004. Spatial synchrony in population dynamics. Annu. Rev. Ecol. Evol. Syst. 35:467–490.

Lima, M., N. C. Stenseth, and F. M. Jaksic. 2002. Population dynamics of a south american rodent: seasonal structure interacting with climate, density dependence and predator effects. Proceedings of the Royal Society of London. Series B: Biological Sciences 269:2579–2586.

Moran, P. A. 1953. The statistical analysis of the canadian lynx cycle. Australian Journal of Zoology 1:291–298.

Nicolau, P. G., R. A. Ims, S. H. Sørbye, and N. G. Yoccoz. 2022. Seasonality, density dependence, and spatial population synchrony. Proceedings of the National Academy of Sciences 119:e2210144119.

Ong, J. J., J. A. Walter, O. P. Jensen, and M. L. Pinsky. 2021. Global hotspots of coherent marine fishery catches. Ecological Applications page e2321.

Peltonen, M., A. M. Liebhold, O. N. Bjørnstad, and D. W. Williams. 2002. Spatial synchrony in forest insect outbreaks: roles of regional stochasticity and dispersal. Ecology 83:3120–3129.

Portmann, R. W., S. Solomon, and G. C. Hegerl. 2009. Spatial and seasonal patterns in climate change, temperatures, and precipitation across the united states. Proceedings of the National Academy of Sciences 106:7324–7329.

Post, E., and M. C. Forchhammer. 2002. Synchronization of animal population dynamics by large-scale climate. Nature 420:168–171.

———. 2004. Spatial synchrony of local populations has increased in association with the recent northern hemisphere climate trend. Proceedings of the National Academy of Sciences 101:9286–9290.

R Core Team. 2021. R: A language and environment for statistical computing .

Rohani, P., D. J. Earn, and B. T. Grenfell. 1999. Opposite patterns of synchrony in sympatric disease metapopulations. Science 286:968–971.

Sawyer, H., A. D. Middleton, M. M. Hayes, M. J. Kauffman, and K. L. Monteith. 2016. The extra mile: Ungulate migration distance alters the use of seasonal range and exposure to anthropogenic risk. Ecosphere 7:e01534.

Schindler, D. E., J. B. Armstrong, and T. E. Reed. 2015. The portfolio concept in ecology and evolution. Frontiers in Ecology and the Environment 13:257–263.

Sheppard, L. W., J. R. Bell, R. Harrington, and D. C. Reuman. 2016. Changes in large-scale climate alter spatial synchrony of aphid pests. Nature Climate Change 6:610–613.

Sheppard, L. W., E. J. Defriez, P. C. Reid, and D. C. Reuman. 2019. Synchrony is more than its top-down and climatic parts: interacting moran effects on phytoplankton in british seas. PLoS computational biology 15:e1006744.

Sinclair, B. J. 1999. Insect cold tolerance: How many kinds of frozen? European Journal of Entomology 96:157–164.

Sinclair, B. J., L. V. Ferguson, G. Salehipour-shirazi, and H. A. MacMillan. 2013. Cross-tolerance and cross-talk in the cold: relating low temperatures to desiccation and immune stress in insects. Integrative and comparative biology 53:545–556.

Stein, M. 1987. Large sample properties of simulations using latin hypercube sampling. Technometrics 29:143–151.

Töpper, J. P., E. Meineri, S. L. Olsen, K. Rydgren, O. Skarpaas, and V. Vandvik. 2018. The devil is in the detail: Nonadditive and context-dependent plant population responses to increasing temperature and precipitation. Global change biology 24:4657–4666.

Viboud, C., O. N. Bjørnstad, D. L. Smith, L. Simonsen, M. A. Miller, and B. T. Grenfell. 2006. Synchrony, waves, and spatial hierarchies in the spread of influenza. science 312:447–451.

Walter, J. A., L. M. Hallett, L. W. Sheppard, T. L. Anderson, L. Zhao, R. J. Hobbs, K. N. Suding, and D. C. Reuman. 2021. Micro-scale geography of synchrony in a serpentine plant community. Journal of Ecology 109:750–762.

Walter, J. A., L. W. Sheppard, T. L. Anderson, J. H. Kastens, O. N. Bjørnstad, A. M. Liebhold, and D. C. Reuman. 2017. The geography of spatial synchrony. Ecology Letters 20:801–814.

Walter, J. A., L. W. Sheppard, P. D. Venugopal, D. C. Reuman, G. Dively, J. F. Tooker, and D. M. Johnson. 2020. Weather and regional crop composition variation drive spatial synchrony of lepidopteran agricultural pests. Ecological Entomology 45:573–582.

Wang, D., T. C. Gouhier, B. A. Menge, and A. R. Ganguly. 2015. Intensification and spatial homogenization of coastal upwelling under climate change. Nature 518:390–394.

Wisnoski, N. I., and J. T. Lennon. 2021. Stabilising role of seed banks and the maintenance of bacterial diversity. Ecology Letters 24:2328–2338.

Tables

Parameter
$f_0 \sim \text{uniform}(0.3, 2.45)$
$k_B \sim \text{uniform}(10, 200)$
$s_0 \sim \text{uniform}(-0.9, 0) \times f_0$
$k_W \sim \text{uniform}(0.1, 1) \times k_B$
$\text{cor}(\epsilon_{B,i}, \epsilon_{B,j}) \sim \text{uniform}(0, 1)$
$\text{cor}(\epsilon_{W,i}, \epsilon_{W,j}) \sim \text{uniform}(0, 1)$
$\text{cor}(\epsilon_B, \epsilon_W) \sim \text{uniform}(-0.5, 0.5)$
$\text{sd}(\epsilon) \sim \text{uniform}(0, 0.1)$
$d \sim \text{uniform}(0, 0.2)$

Table 1: Distributions from which parameters were drawn for sensitivity testing.

Figure 1: Results from analytical solution (eqn. 10) showing how population spatial synchrony depends on various parameters. a) The effects of varying breeding season ($\mathrm{cor}(\epsilon_{b,i}, \epsilon_{b,j})$) and overwintering season ($\mathrm{cor}(\epsilon_{w,i}, \epsilon_{w,j})$) synchrony. Both varied from 0 to 1 with all other parameters held constant at $f_0 = 1.6$, $k_B = 100$, $s_0 = 0$, $k_W = 50$, $\mathrm{cor}(\epsilon_B, \epsilon_W) = 0.2$, and $\sigma = 0.01$. b) The effects of varying cross season synchrony ($-0.5 \leq \mathrm{cor}(\epsilon_B, \epsilon_W) \leq 0.5$) with other parameters held constant at $k_B = 100$, $k_W = 85$, $\mathrm{cor}(\epsilon_{B,i}, \epsilon_{B,j}) = 0.3$, $\mathrm{cor}(\epsilon_{W,i}, \epsilon_{W,j}) = 0.1$, and $\sigma = 0.05$. Black: $f_0 = 1.2$ and $\hat{s}_0 = -0.4$, blue: $f_0 = 1.8$ and $\hat{s}_0 = 0.0$, red: $f_0 = 2.4$ and $\hat{s}_0 = -0.1$, and green: $f_0 = 0.6$ and $\hat{s}_0 = -0.7$. c) The effects of varying growth rate (f_0) and relative survival ($\hat{s}_0$), which varied from $0.3 \leq f_0 \leq 2.45$ and $-0.9 \leq \hat{s}_0 \leq 0$ with other parameters held constant at $k_B = 100$, $k_W = 85$, $\mathrm{cor}(\epsilon_{B,i}, \epsilon_{B,j}) = 0.8$, $\mathrm{cor}(\epsilon_{W,i}, \epsilon_{W,j}) = 0.2$, $\mathrm{cor}(\epsilon_B, \epsilon_W) = 0.0$, and $\sigma = 0.05$.

Figure 2: Spatial synchrony depends on f_0, $\hat{s}_0$, $\mathrm{cor}(\epsilon_{B,i}, \epsilon_{B,j})$, and $\mathrm{cor}(\epsilon_{W,i}, \epsilon_{W,j})$. a) All else being equal, varying f_0 and $\hat{s}_0$ changes population growth from an undercompensatory to an overcompensatory regime. b)-g) show the effect of f_0 and s_0 on predicted population spatial synchrony (eqn. 10) with the spatial synchrony of environmental drivers at the indicated values. In the undercompensatory regime, increasing f_0 or $\hat{s}_0$ tends to increase spatial synchrony, but in the overcompensatory regime increasing f_0 or $\hat{s}_0$ tends to decrease spatial synchrony. For all panels, $k_B = 100$, $k_W = 85$, $\mathrm{cor}(\epsilon_B, \epsilon_W) = 0.0$, and $\sigma = 0.05$.

Figure 3: Sensitivity of spatial synchrony of population size ($\mathrm{cor}(N_i(t), N_j(t))$) from the main, no overwintering, and same environment simulation models to variation in model parameters, as represented in coefficients from multiple linear regression on standardized predictor variables. Parameter values were drawn from distributions given in Table 1. Simulations giving rise to undercompensatory versus overcompensatory population growth were separated given the findings in Figure 2. Parameter combinations resulting in undercompensatory versus overcompensatory population growth were determined from the deterministic skeleton of our stochastic model.

Figure 4: Population spatial synchrony ($\mathrm{cor}(N_i(t), N_j(t))$) as a function of environmental synchrony and population growth regime for the main, no overwintering, and same environment simulation models. In a, b, d, e, the color scale corresponds to $\mathrm{cor}(N_i(t), N_j(t))$. Here, $f_0 = 1$ for undercompensatory dynamics and $f_0 = 2$ for overcompensatory dynamics, $k_B = 100$, $\hat{s_0} = -0.1$, $k_W = 80$, $\mathrm{cor}(\epsilon_B, \epsilon_W) = 0.2$, and $\mathrm{sd}(\epsilon) = 0.1$.

Figure 5: Population synchrony when measured between overwintering and breeding [i.e., $N_i(t)$; a), d)] versus when measured at the end of the breeding season [i.e., $B_i(t)$; b, e)] for the main model for population growth in undercompensatory and overcompensatory regimes; differences are shown in c), f). Here, $f_0 = 1$ for undercompensatory dynamics and $f_0 = 2$ for overcompensatory dynamics, $k_B = 100$, $\hat{s_0} = -0.1$, $k_W = 80$, $\mathrm{cor}(\epsilon_B, \epsilon_W) = 0.2$, and $\mathrm{sd}(\epsilon) = 0.1$.

Figure 1

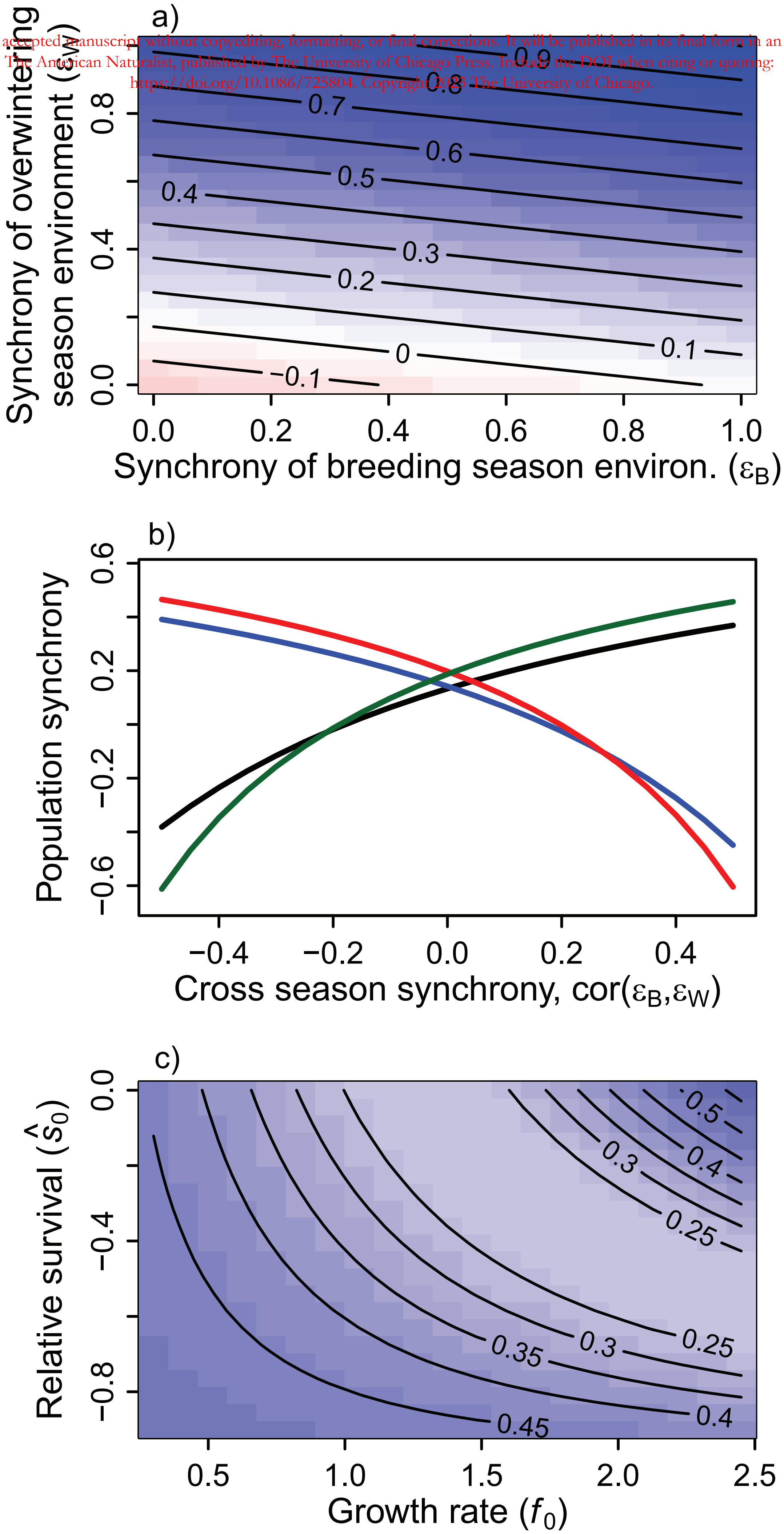
a)
Synchrony of overwintering season environment (ε_W)
0.0
0.4
0.8
0.9
0.8
0.7
0.6
0.5
0.4
0.3
0.2
0.1
0
−0.1
0.0
0.2
0.4
0.6
0.8
1.0
Synchrony of breeding season environ. (ε_B)
b)
Population synchrony
0.6
0.2
−0.2
−0.6
−0.4
−0.2
0.0
0.2
0.4
Cross season synchrony, cor(ε_B,ε_W)
c)
Relative survival ($\hat{s}_0$)
0.0
−0.4
−0.8
0.5
0.4
0.3
0.25
0.35
0.3
0.25
0.45
0.4
0.5
1.0
1.5
2.0
2.5
Growth rate (f_0)

Figure 2 (print only)

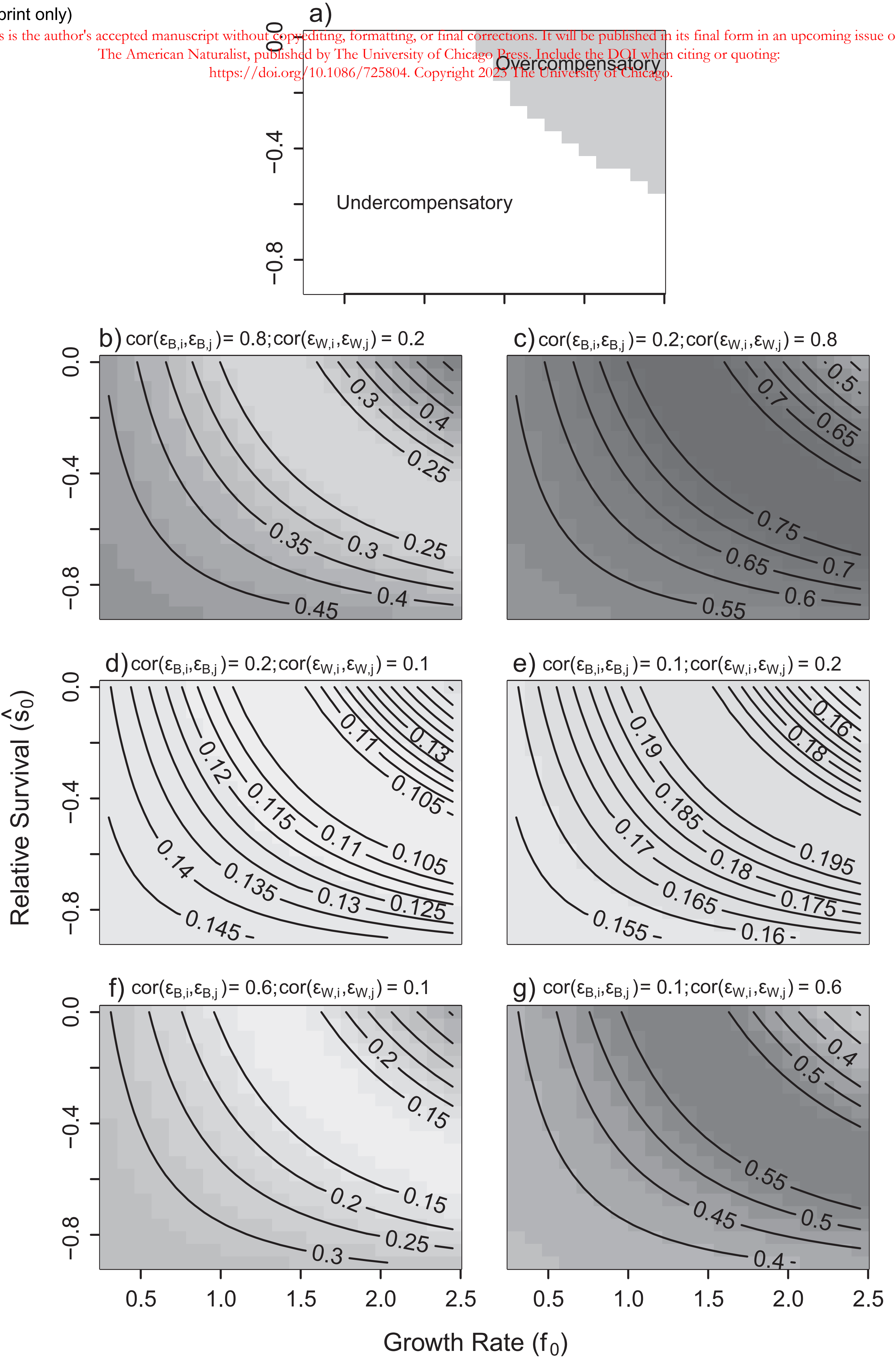

Figure 2

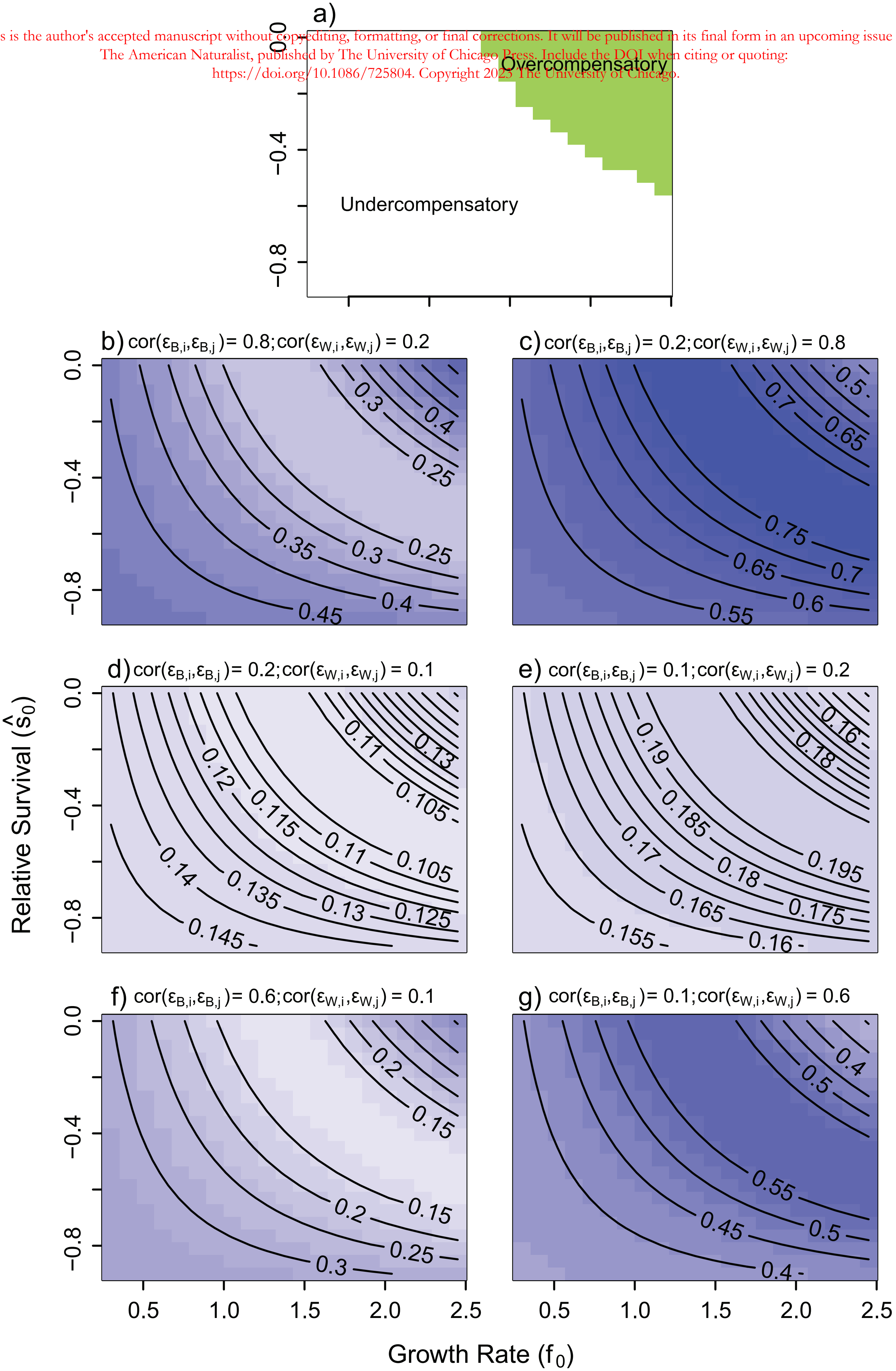
a)
Overcompensatory
Undercompensatory
0.0
−0.4
−0.8
b) $cor(\varepsilon_{B,i},\varepsilon_{B,j}) = 0.8; cor(\varepsilon_{W,i},\varepsilon_{W,j}) = 0.2$
0.3
0.4
0.25
0.35
0.3
0.25
0.45
0.4
c) $cor(\varepsilon_{B,i},\varepsilon_{B,j}) = 0.2; cor(\varepsilon_{W,i},\varepsilon_{W,j}) = 0.8$
0.5
0.7
0.65
0.75
0.65
0.7
0.55
0.6
d) $cor(\varepsilon_{B,i},\varepsilon_{B,j}) = 0.2; cor(\varepsilon_{W,i},\varepsilon_{W,j}) = 0.1$
0.11
0.13
0.105
0.12
0.115
0.11
0.105
0.14
0.135
0.13
0.125
0.145
e) $cor(\varepsilon_{B,i},\varepsilon_{B,j}) = 0.1; cor(\varepsilon_{W,i},\varepsilon_{W,j}) = 0.2$
0.19
0.16
0.18
0.185
0.17
0.18
0.195
0.165
0.175
0.155
0.16
f) $cor(\varepsilon_{B,i},\varepsilon_{B,j}) = 0.6; cor(\varepsilon_{W,i},\varepsilon_{W,j}) = 0.1$
0.2
0.15
0.2
0.15
0.25
0.3
g) $cor(\varepsilon_{B,i},\varepsilon_{B,j}) = 0.1; cor(\varepsilon_{W,i},\varepsilon_{W,j}) = 0.6$
0.4
0.5
0.55
0.45
0.5
0.4
Relative Survival ($\hat{s}_0$)
Growth Rate (f_0)
0.5
1.0
1.5
2.0
2.5

Figure 3

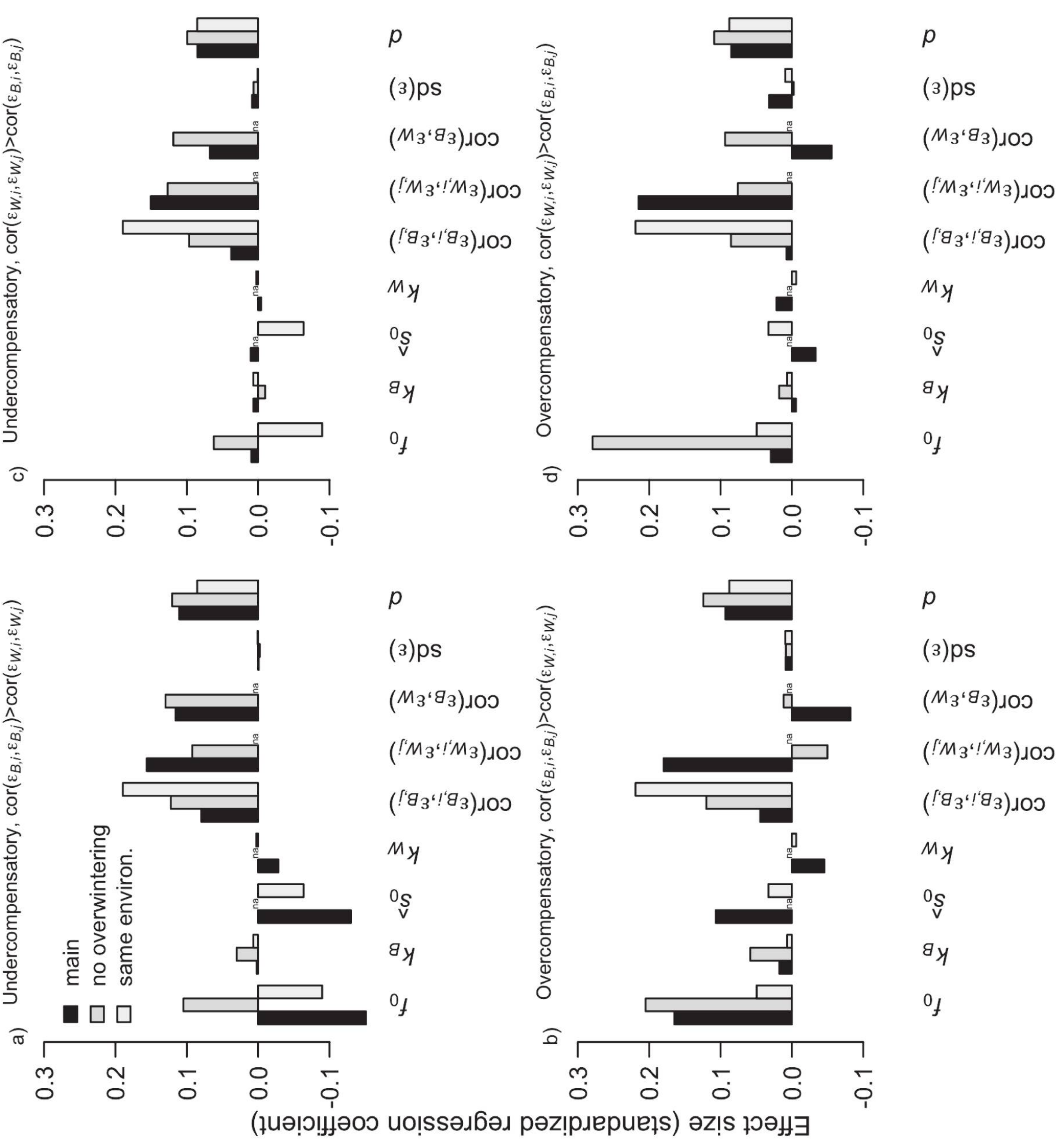
a)
Undercompensatory, $cor(\varepsilon_{B,i},\varepsilon_{B,j})>cor(\varepsilon_{W,i},\varepsilon_{W,j})$
b)
Overcompensatory, $cor(\varepsilon_{B,i},\varepsilon_{B,j})>cor(\varepsilon_{W,i},\varepsilon_{W,j})$
c)
Undercompensatory, $cor(\varepsilon_{W,i},\varepsilon_{W,j})>cor(\varepsilon_{B,i},\varepsilon_{B,j})$
d)
Overcompensatory, $cor(\varepsilon_{W,i},\varepsilon_{W,j})>cor(\varepsilon_{B,i},\varepsilon_{B,j})$
main
no overwintering
same environ.
Effect size (standardized regression coefficient)
0.3
0.2
0.1
0.0
-0.1
f_0
k_B
$\hat{s}_0$
k_W
$cor(\varepsilon_{B,i},\varepsilon_{B,j})$
$cor(\varepsilon_{W,i},\varepsilon_{W,j})$
$cor(\varepsilon_B,\varepsilon_W)$
$sd(\varepsilon)$
d
na

Figure 4

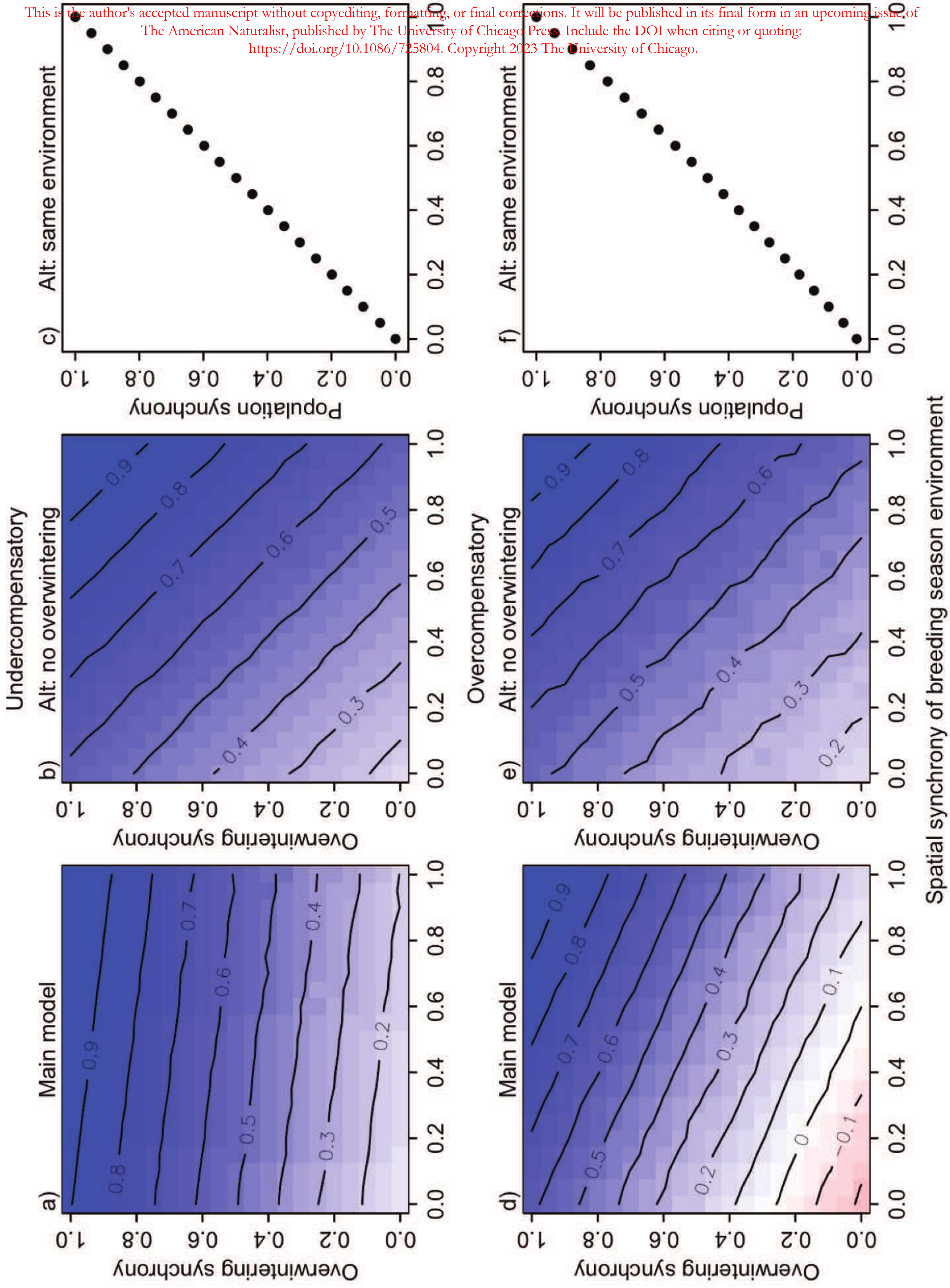
Undercompensatory
Overcompensatory
a) Main model
b) Alt: no overwintering
c) Alt: same environment
d) Main model
e) Alt: no overwintering
f) Alt: same environment
Overwintering synchrony
Population synchrony
Spatial synchrony of breeding season environment
0.0
0.2
0.4
0.6
0.8
1.0
0.9
0.8
0.7
0.6
0.5
0.4
0.3
0.2
0.1
0
-0.1

Figure 5

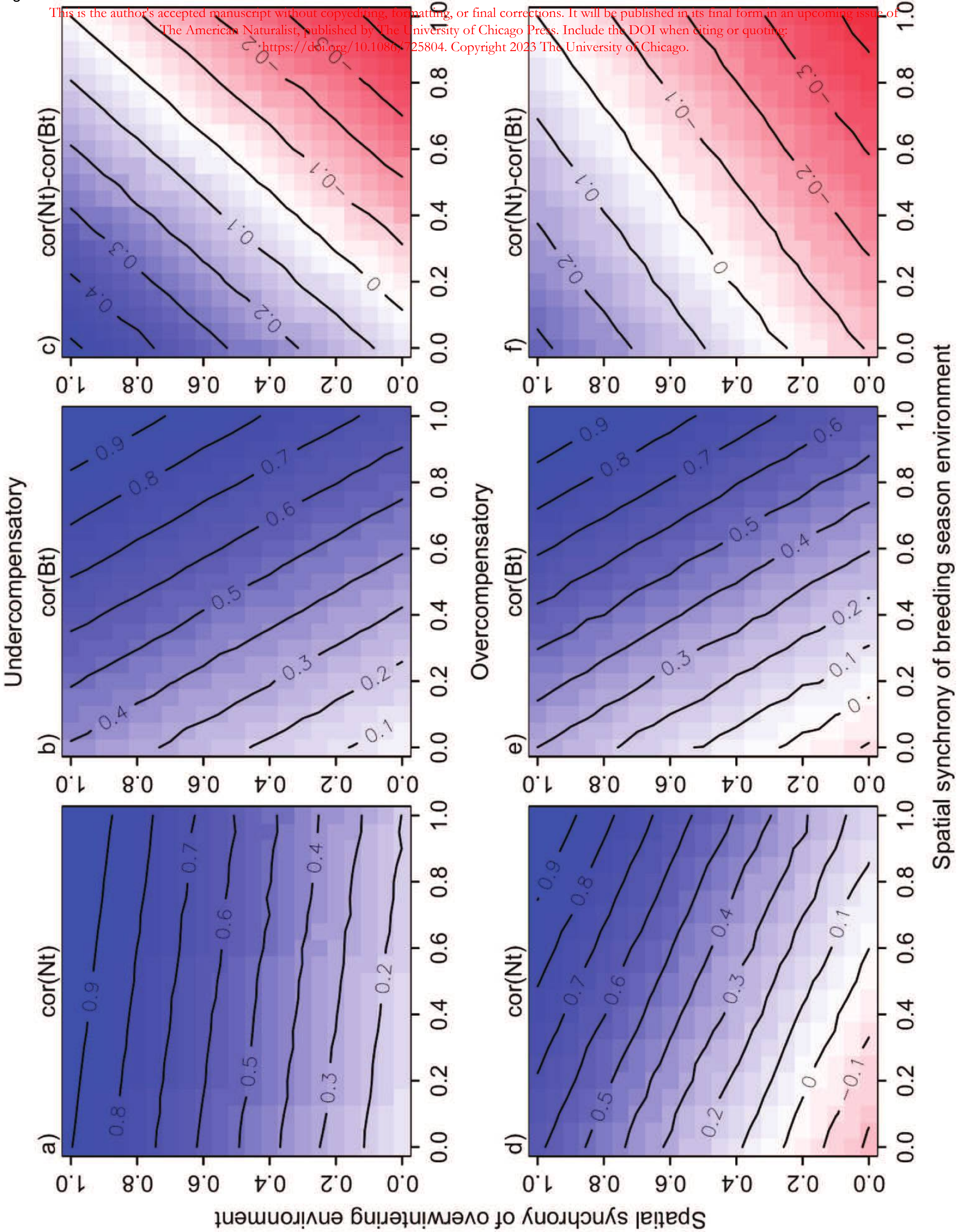
Undercompensatory
Overcompensatory
a)
cor(Nt)
b)
cor(Bt)
c)
cor(Nt)-cor(Bt)
d)
cor(Nt)
e)
cor(Bt)
f)
cor(Nt)-cor(Bt)
0.0
0.2
0.4
0.6
0.8
1.0
0.9
0.8
0.7
0.6
0.5
0.4
0.3
0.2
0.1
0
-0.1
-0.2
-0.3
Spatial synchrony of overwintering environment
Spatial synchrony of breeding season environment

Online supplement to: Seasonality alters population spatial synchrony – *The American Naturalist*

Jonathan A. Walter[1,2∗], Daniel C. Reuman[3], Kimberly R. Hall[4], Herman H. Shugart[1], Lauren G. Shoemaker[5]

1. Department of Environmental Sciences, University of Virginia, Charlottesville, Virginia 22904;

2. Center for Watershed Sciences, University of California, Davis, California 95616;

3. Department of Ecology and Evolutionary Biology & Center for Ecological Research, University of Kansas, Lawrence, Kansas 66047;

4. North America Science, The Nature Conservancy, Haslett, Michigan 48840;

5. Botany Department, University of Wyoming, Laramie, Wyoming 82071;

∗ Corresponding author; e-mail: jawalter@ucdavis.edu.

A: Details of analytical derivation

To compute synchrony of the linearized model (eq. 6), we compute $\mathrm{cor}(n_i, n_j)$ for $i \neq j$ by computing $\mathrm{cov}(n_i, n_j)$, $\mathrm{var}(n_i)$ and $\mathrm{var}(n_j)$. We have

$$\mathrm{cov}(n_i(t), n_j(t)) = \mathrm{cov}(P_A n_i(t-1) + P_B e_{B,i}(t) + P_W e_{W,i}(t), P_A n_j(t-1) + P_B e_{B,j}(t) + P_W e_{W,j}(t)) \tag{S.1}$$

$$= P_A^2 \, \mathrm{cov}(n_i(t-1), n_j(t-1)) \tag{S.2}$$

$$+ P_B^2 \, \mathrm{cov}(\epsilon_{B,i}(t), \epsilon_{B,j}(t)) \tag{S.3}$$

$$+ P_W^2 \, \mathrm{cov}(\epsilon_{W,i}(t), \epsilon_{W,j}(t)) \tag{S.4}$$

$$+ 2 P_B P_W \, \mathrm{cov}(\epsilon_{B,i}(t), \epsilon_{W,j}(t)). \tag{S.5}$$

We here used some of the assumptions about the environmental noise random variables described in the main text. We then have

$$(1 - P_A^2) \, \mathrm{cov}(n_i, n_j) = P_B^2 \, \mathrm{cov}(\epsilon_{B,i}, \epsilon_{B,j}) + P_W^2 \, \mathrm{cov}(\epsilon_{W,i}, \epsilon_{W,j}) + 2 P_B P_W \, \mathrm{cov}(\epsilon_{B,i}, \epsilon_{W,j}). \tag{S.6}$$

Furthermore,

$$\mathrm{var}(n_i(t)) = P_A^2 \, \mathrm{var}(n_i(t-1)) + P_B^2 \, \mathrm{var}(\epsilon_{B,i}(t)) + P_W^2 \, \mathrm{var}(\epsilon_{W,i}(t)) + 2 P_B P_W \, \mathrm{cov}(\epsilon_{B,i}(t), \epsilon_{W,i}(t)), \tag{S.7}$$

and therefore

$$(1 - P_A^2) \, \mathrm{var}(n_i) = P_B^2 \, \mathrm{var}(\epsilon_{B,i}) + P_W^2 \, \mathrm{var}(\epsilon_{W,i}) + 2 P_B P_W \, \mathrm{cov}(\epsilon_{B,i}, \epsilon_{W,i}), \tag{S.8}$$

which holds independently of the value of i. Therefore,

$$\mathrm{cor}(n_i, n_j) = \frac{P_B^2 \, \mathrm{cov}(\epsilon_{B,i}, \epsilon_{B,j}) + P_W^2 \, \mathrm{cov}(\epsilon_{W,i}, \epsilon_{W,j}) + 2 P_B P_W \, \mathrm{cov}(\epsilon_{B,i}, \epsilon_{W,j})}{P_B^2 \, \mathrm{var}(\epsilon_{B,i}) + P_W^2 \, \mathrm{var}(\epsilon_{W,i}) + 2 P_B P_W \, \mathrm{cov}(\epsilon_{B,i}, \epsilon_{W,i})}. \tag{S.9}$$

The correlation $\mathrm{cor}(n_i, n_j)$ approximately equals the correlation $\mathrm{cor}(N_i, N_j)$ of the original (unlinearized) model, therefore:

$$\mathrm{cor}(N_i, N_j) \approx \frac{P_B^2 \,\mathrm{cov}(\epsilon_{B,i}, \epsilon_{B,j}) + P_W^2 \,\mathrm{cov}(\epsilon_{W,i}, \epsilon_{W,j}) + 2P_B P_W \,\mathrm{cov}(\epsilon_{B,i}, \epsilon_{W,j})}{P_B^2 \,\mathrm{var}(\epsilon_{B,i}) + P_W^2 \,\mathrm{var}(\epsilon_{W,i}) + 2P_B P_W \,\mathrm{cov}(\epsilon_{B,i}, \epsilon_{W,i})}. \tag{S.10}$$

Note that the first two terms in the numerator relate to traditional measures of spatial synchrony of environmental variables, but “cross-variable” synchrony, both between and within locations (in the numerator and denominator, respectively), also contribute.

To estimate $\mathrm{cor}(N_i, N_j)$ for our chosen instance of this general model (eqs. 11 and 12), using eq. S.10, we must compute the partial derivatives P_B, and P_W at the equilibrium population density N^*, and the expected values of the environmental drivers $\overline{\epsilon}_B$ and $\overline{\epsilon}_B$:

$$\begin{aligned} P_B =& [N^* \exp(f_0) \exp(-N^*/k_B) \exp(\epsilon_B) \exp(s_0) \cdot \\ & exp(-(N^* \exp(f_0) \exp(-N^*/k_B) \exp(\epsilon_B))/k_W) - \\ & N^* \exp(f_0) \exp(-N^*/k_B) \exp(\epsilon_B) \exp(s_0) \cdot \\ & (\exp(-(N^* \exp(f_0) \exp(-N *^/\, k_B) \exp(eB))/kW) \cdot \\ & (N^* \exp(f_0) \exp(-N^*/k_B) \exp(\epsilon_B)/k_W))] \cdot \exp(\epsilon_W), \end{aligned} \tag{S.11}$$

$$\begin{aligned} P_W =& N^* \exp(f_0) \exp(-N^*/k_B) \exp(\epsilon_B) \exp(s_0) \cdot \\ & \exp[-(N^* \exp(f_0) \exp(-N^*/k_B) \exp(\epsilon_B))/k_W] \exp(\epsilon_W). \end{aligned} \tag{S.12}$$

B: Exploration of cross-variable synchrony

To explore general patterns of cross-variable synchrony, we measured the Pearson correlation between summertime (June, July, August) and wintertime (December, January, February) daily mean temperatures in the conterminous United States, and between summertime temperatures and wintertime precipitation. 1990-2009 monthly mean temperature and total precipitation time series were extracted from PRISM gridded climate data (https://prism.oregonstate.edu) at 1000 randomly selected locations and aggregated into annual-time-step summer and winter time series by averaging. We computed the cross-correlation (i.e., $\text{cor}(T_{summer}(i), T_{winter}(j))$ between summer and winter temperatures for all site pairs, including the cross-correlation between summer and winter temperature in the same location, i.e., $i = j$. Prior to analysis, linear trends were removed from all time series. For summer and winter temperatures, cross-season synchrony in the same location tended to be low (median = 0.027), but could take moderately positive and negative values (2.5% quantile = -0.35, 97.5% quantile = 0.45). The distribution of cross-season synchrony between different locations had a similar distribution (median = 0.044; 2.5% quantile = -0.41, 97.5% quantile = 0.48). For summer temperature and winter precipitation, cross-season synchrony in the same location tended to be somewhat negative (median = -0.14), and could take moderately positive and negative values (2.5% quantile = -0.51, 97.5% quantile = 0.32). The distribution of cross-season synchrony between different locations had a similar distribution (median = -0.11; 2.5% quantile = -0.65, 97.5% quantile = 0.44). Although cross-season synchrony was commonly low, moderate values were relatively common, and very high values, up to ±0.8, were observed, though very rarely.

C: Supplemental Figures

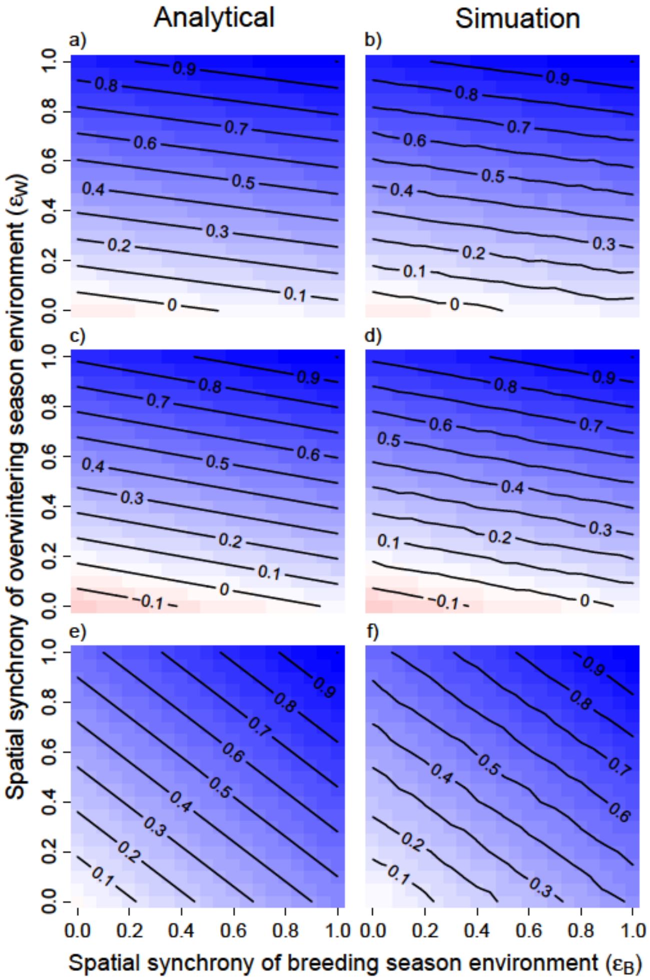

Figure S.1: Comparison of analytical (left column) and simulation (right column) calculations of spatial synchrony. In all cases, breeding season ($\mathrm{cor}(\epsilon_{B,i}, \epsilon_{B,j})$) and overwintering season ($\mathrm{cor}(\epsilon_{W,i}, \epsilon_{W,j})$) synchrony both varied from 0 to 1. All other parameters were held constant at (a-b): $f_0 = 1.05$, $k_B = 50$, $s_0 = -0.2$, $k_W = 40$, $\mathrm{cor}(\epsilon_B, \epsilon_W) = -0.1$, and $\sigma = 0.02$; (c-d): $f_0 = 1.6$, $k_B = 100$, $s_0 = 0$, $k_W = 50$, $\mathrm{cor}(\epsilon_B, \epsilon_W) = 0.2$, and $\sigma = 0.01$; (e-f): $f_0 = 2.2$, $k_B = 100$, $s_0 = -0.1$, $k_W = 80$, $\mathrm{cor}(\epsilon_B, \epsilon_W) = 0$, and $\sigma = 0.1$.

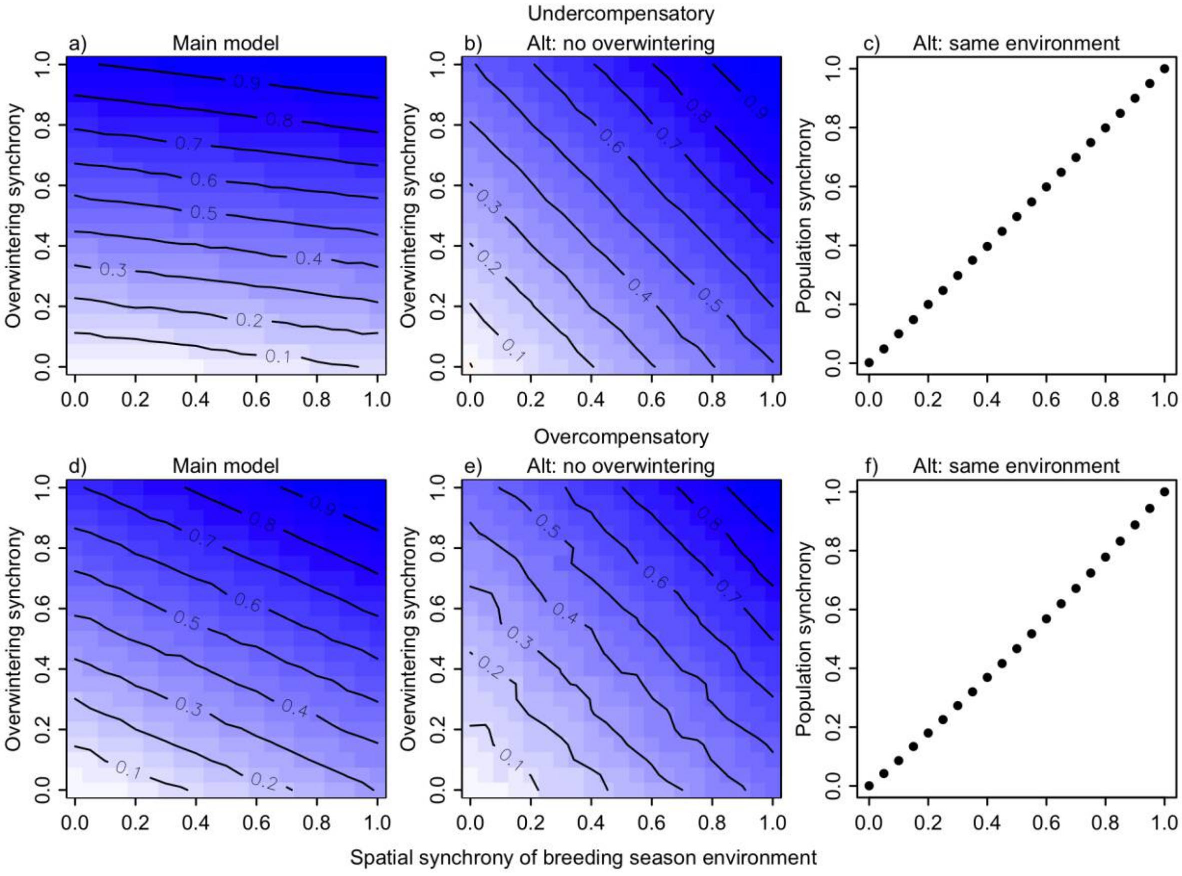

Figure S.2: Population spatial synchrony ($\mathrm{cor}(N_i(t), N_j(t))$) as a function of environmental synchrony and population growth regime for the main, no overwintering, and same environment simulation models. In a, b, d, e, the color scale corresponds to $\mathrm{cor}(N_i(t), N_j(t))$. Parameter values are as in main text Figure 4, except $\mathrm{cor}(\epsilon_B, \epsilon_W) = 0$.

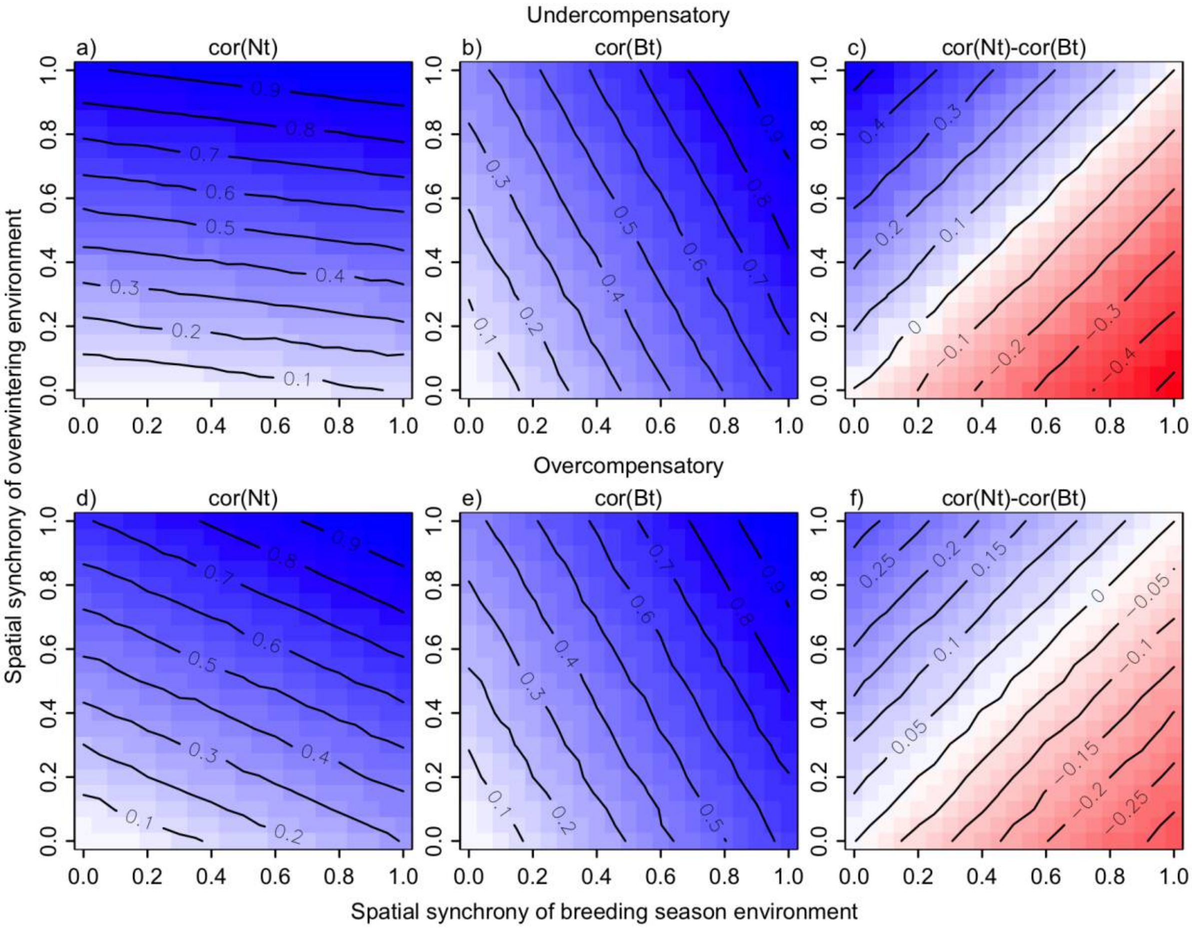

Figure S.3: Population synchrony when measured between overwintering and breeding [i.e., $N_i(t)$; a), d)] versus when measured at the end of the breeding season [i.e., $B_i()$; b, e)] for the main model for population growth in undercompensatory and overcompensatory regimes; differences are shown in c), f). Parameter values are as in main text Figure 5, except $\text{cor}(\epsilon_B, \epsilon_W) = 0$.

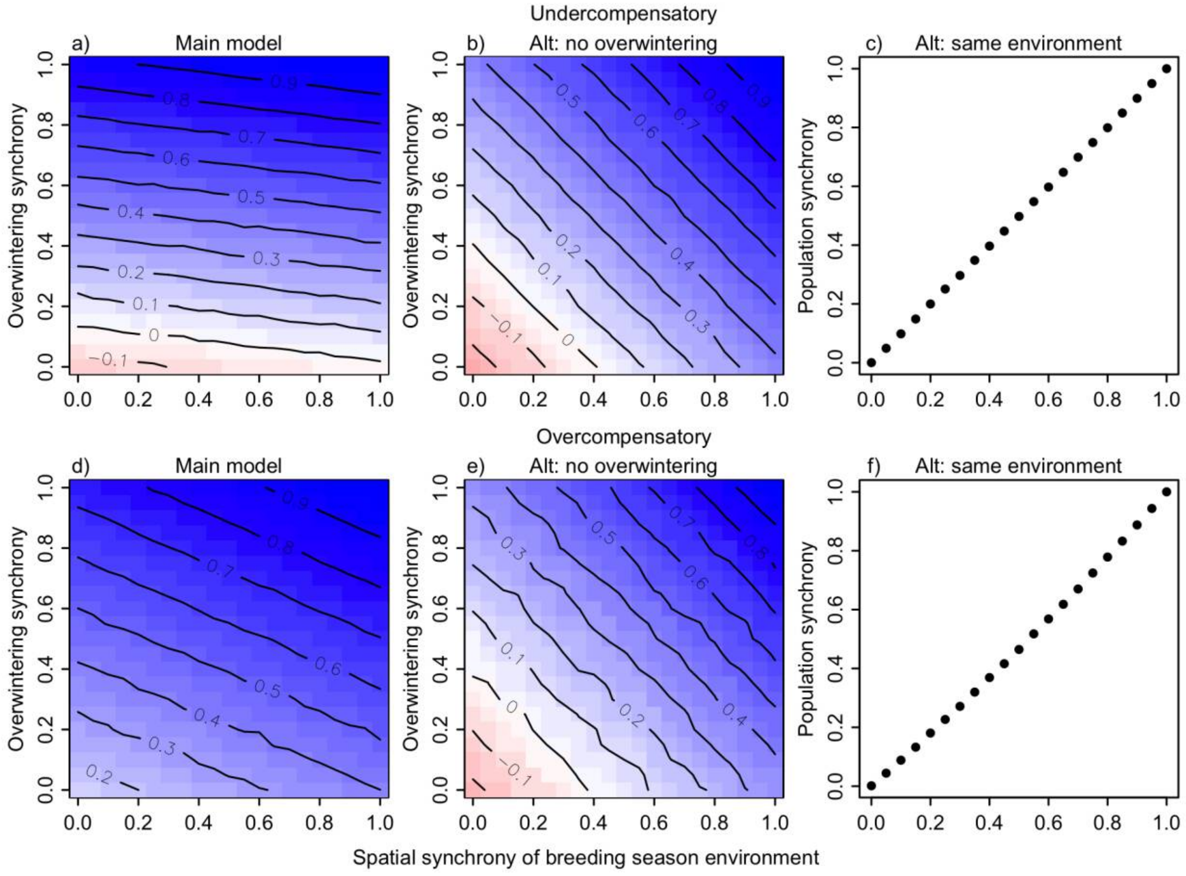

Figure S.4: Population spatial synchrony (cor$(N_i(t), N_j(t))$) as a function of environmental synchrony and population growth regime for the main, no overwintering, and same environment simulation models. In a, b, d, e, the color scale corresponds to cor$(N_i(t), N_j(t))$. Parameter values are as in main text Figure 4, except cor$(\epsilon_B, \epsilon_W) = -0.2$.

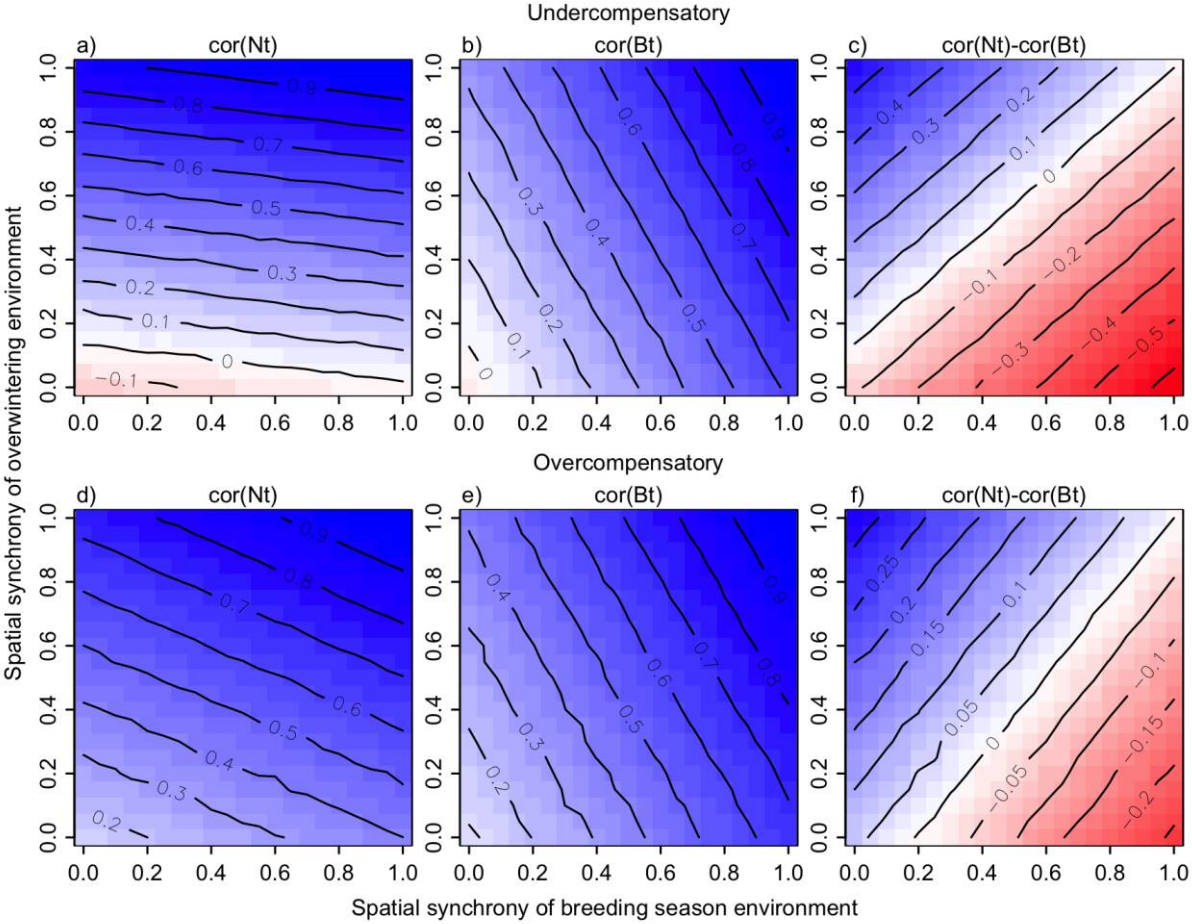

Figure S.5: Population synchrony when measured between overwintering and breeding [i.e., $N_i(t)$; a), d)] versus when measured at the end of the breeding season [i.e., $B_i()$; b, e)] for the main model for population growth in undercompensatory and overcompensatory regimes; differences are shown in c), f). Parameter values are as in main text Figure 5, except $\mathrm{cor}(\epsilon_B, \epsilon_W) = -0.2$.

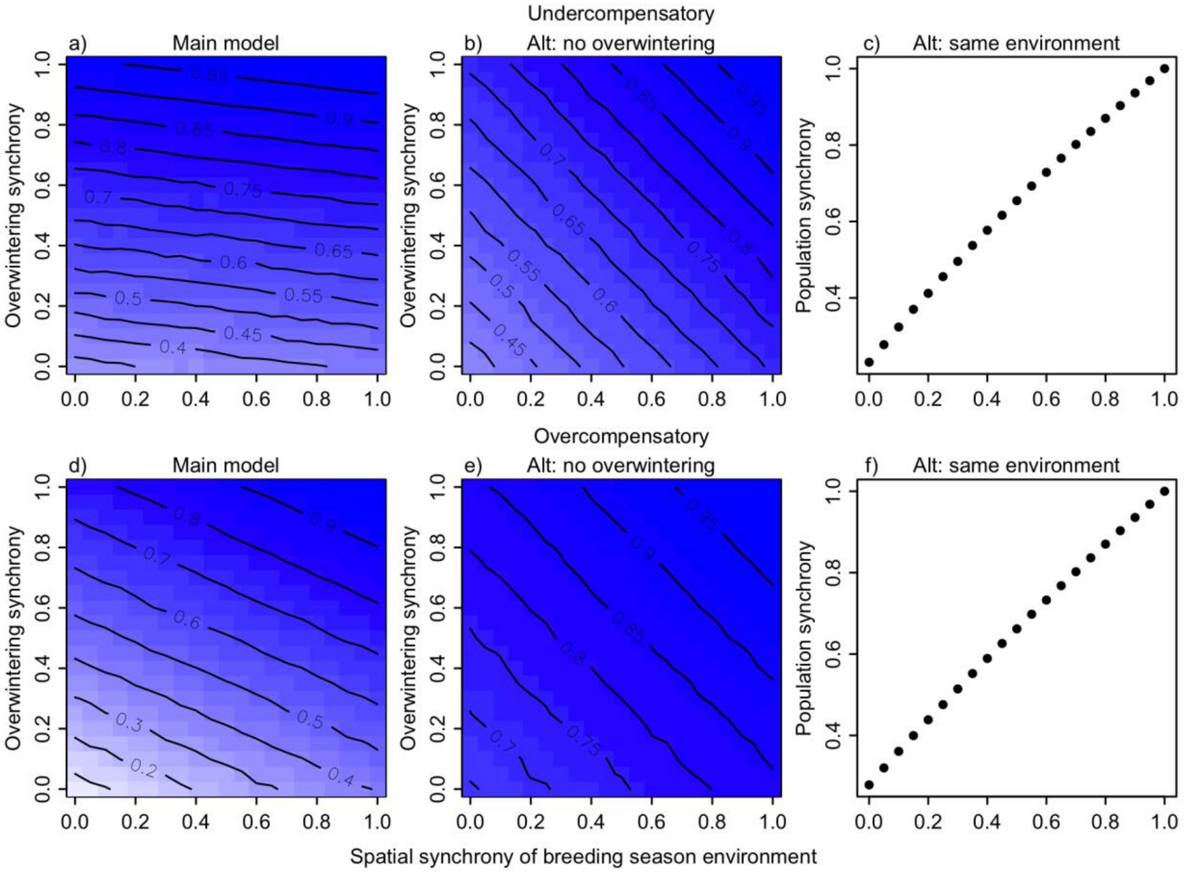

Figure S.6: Population spatial synchrony $(\mathrm{cor}(N_i(t), N_j(t)))$ as a function of environmental synchrony and population growth regime for the main, no overwintering, and same environment simulation models. In a, b, d, e, the color scale corresponds to $\mathrm{cor}(N_i(t), N_j(t))$. Parameter values are as in main text Figure 4, except the dispersal rate d is 0.1.

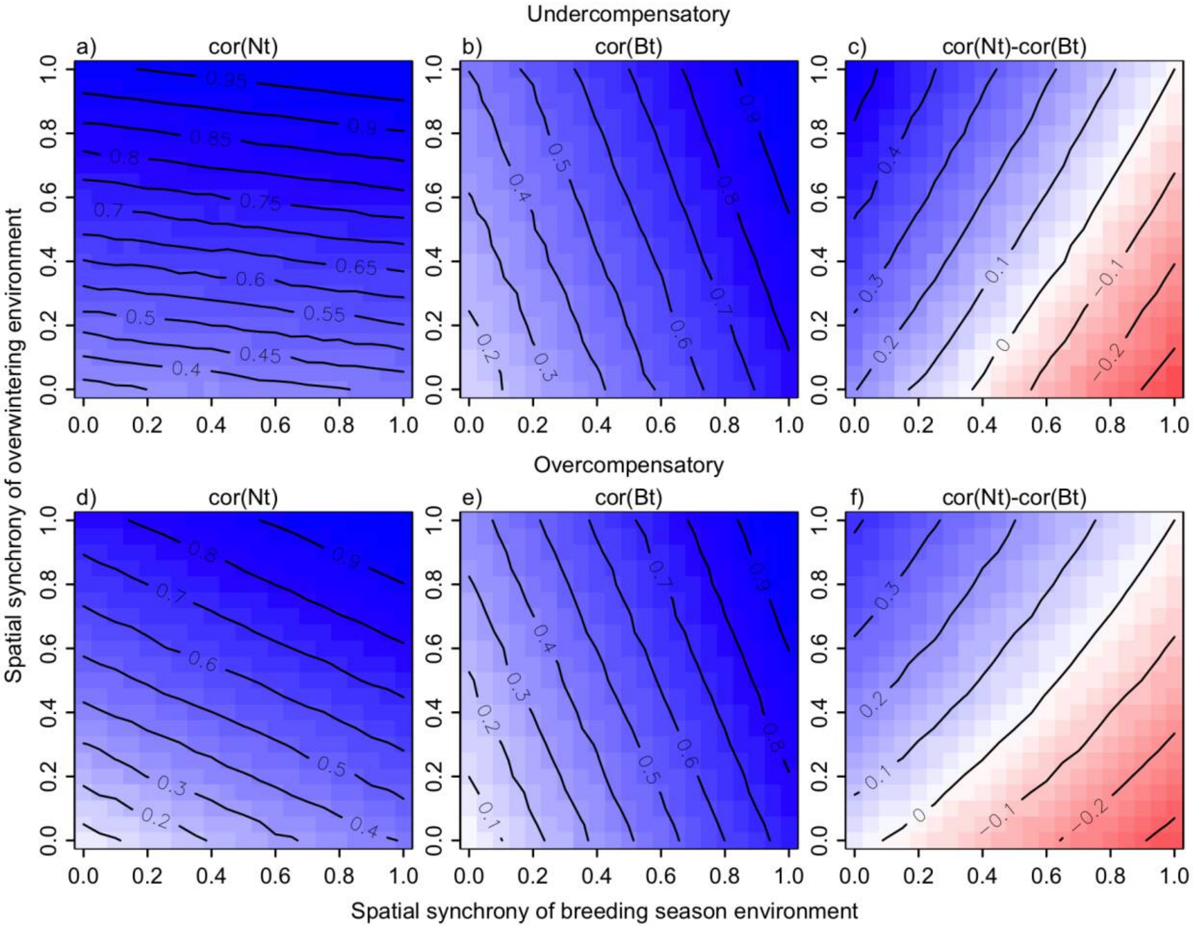

Figure S.7: Population synchrony when measured between overwintering and breeding [i.e., $N_i(t)$; a), d)] versus when measured at the end of the breeding season [i.e., $B_i()$; b, e)] for the main model for population growth in undercompensatory and overcompensatory regimes; differences are shown in c), f). Parameter values are as in main text Figure 5, except the dispersal rate d is 0.1.

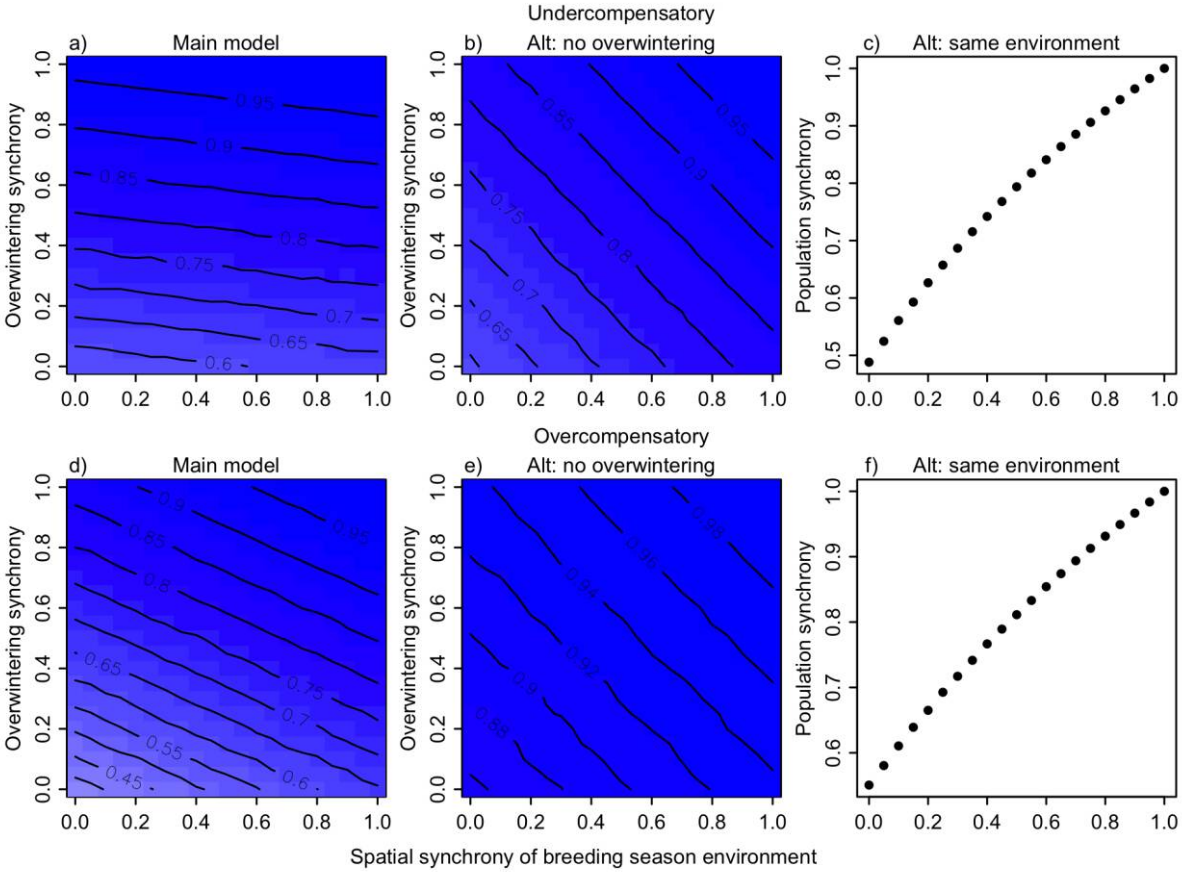

Figure S.8: Population spatial synchrony ($\mathrm{cor}(N_i(t), N_j(t))$) as a function of environmental synchrony and population growth regime for the main, no overwintering, and same environment simulation models. In a, b, d, e, the color scale corresponds to $\mathrm{cor}(N_i(t), N_j(t))$. Parameter values are as in main text Figure 4, except the dispersal rate d is 0.2.

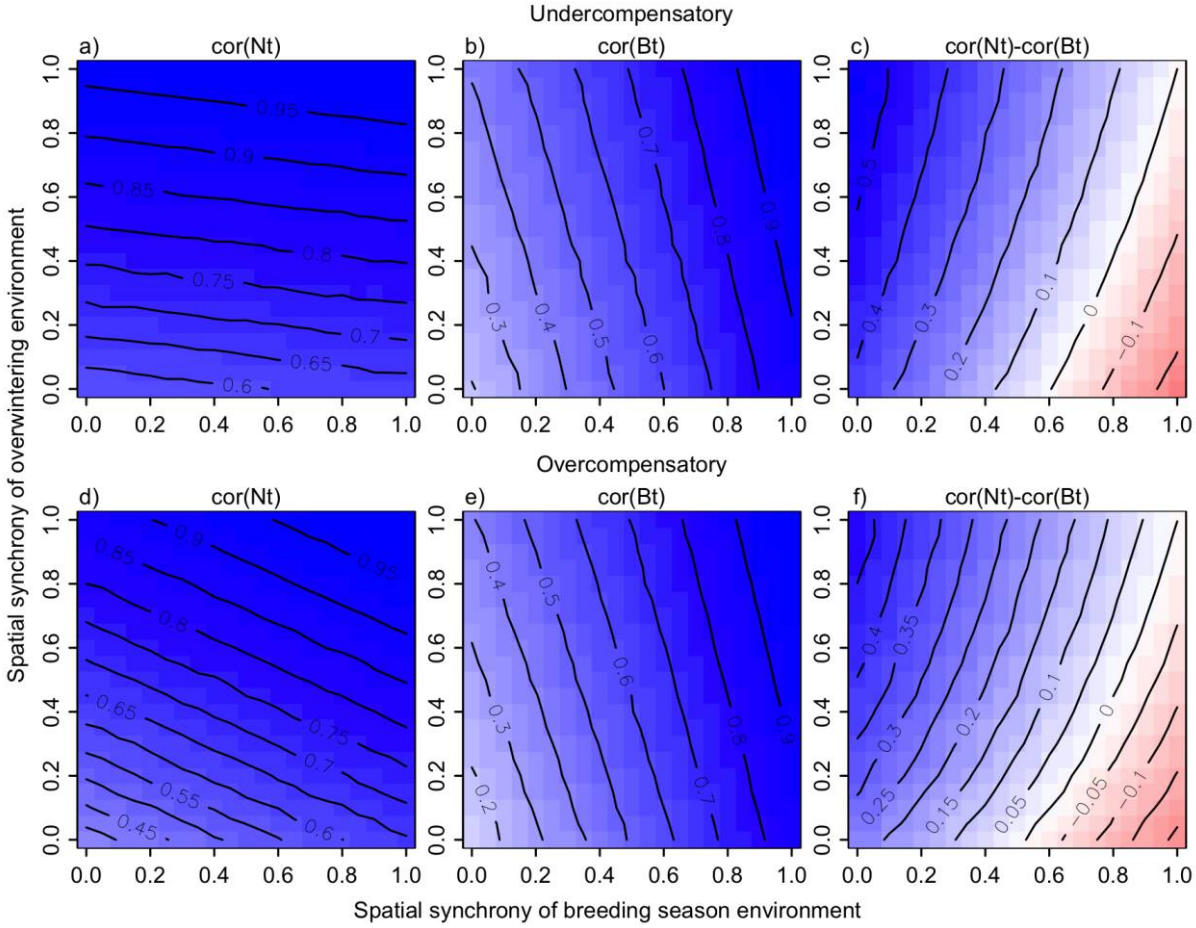

Figure S.9: Population synchrony when measured between overwintering and breeding [i.e., $N_i(t)$; a), d)] versus when measured at the end of the breeding season [i.e., $B_i()$; b, e)] for the main model for population growth in undercompensatory and overcompensatory regimes; differences are shown in c), f). Parameter values are as in main text Figure 5, except the dispersal rate d is 0.2.

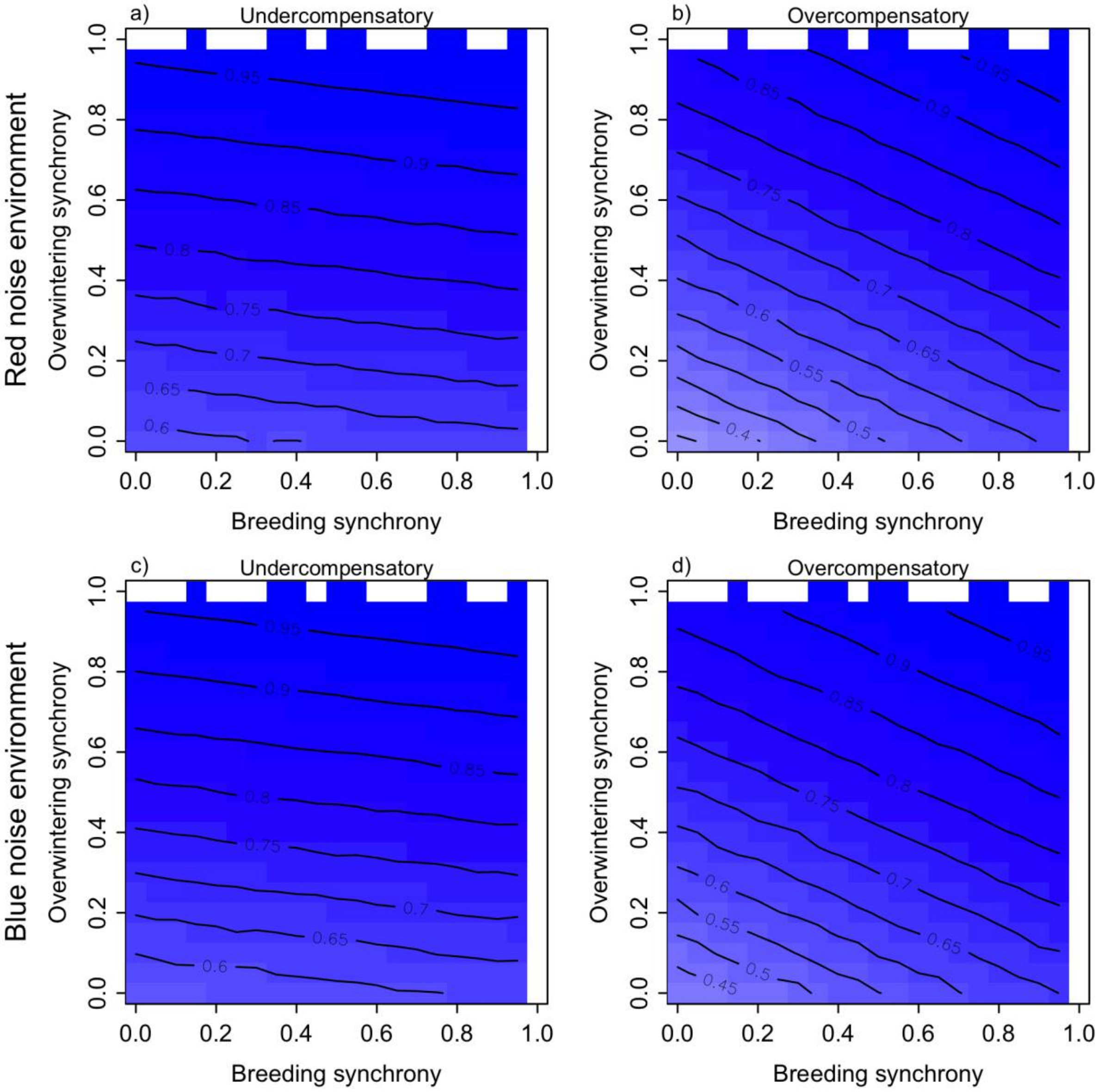

Figure S.10: Population synchrony ($cor(N_i(t), N_j(t))$) when the environmental drivers exhibit interannual correlation. The ”red noise” environments have positive lag-1 autocorrelation (0.2) and the ”blue noise” environments have negative lag-1 autocorrelation (-0.2). Parameter values are as in main text Figure 5 otherwise. Missing data corresponds to edge case parameter combinations for which the environmental driver covariance matrix was not positive-definite, causing technical challenges with generating driver time series.

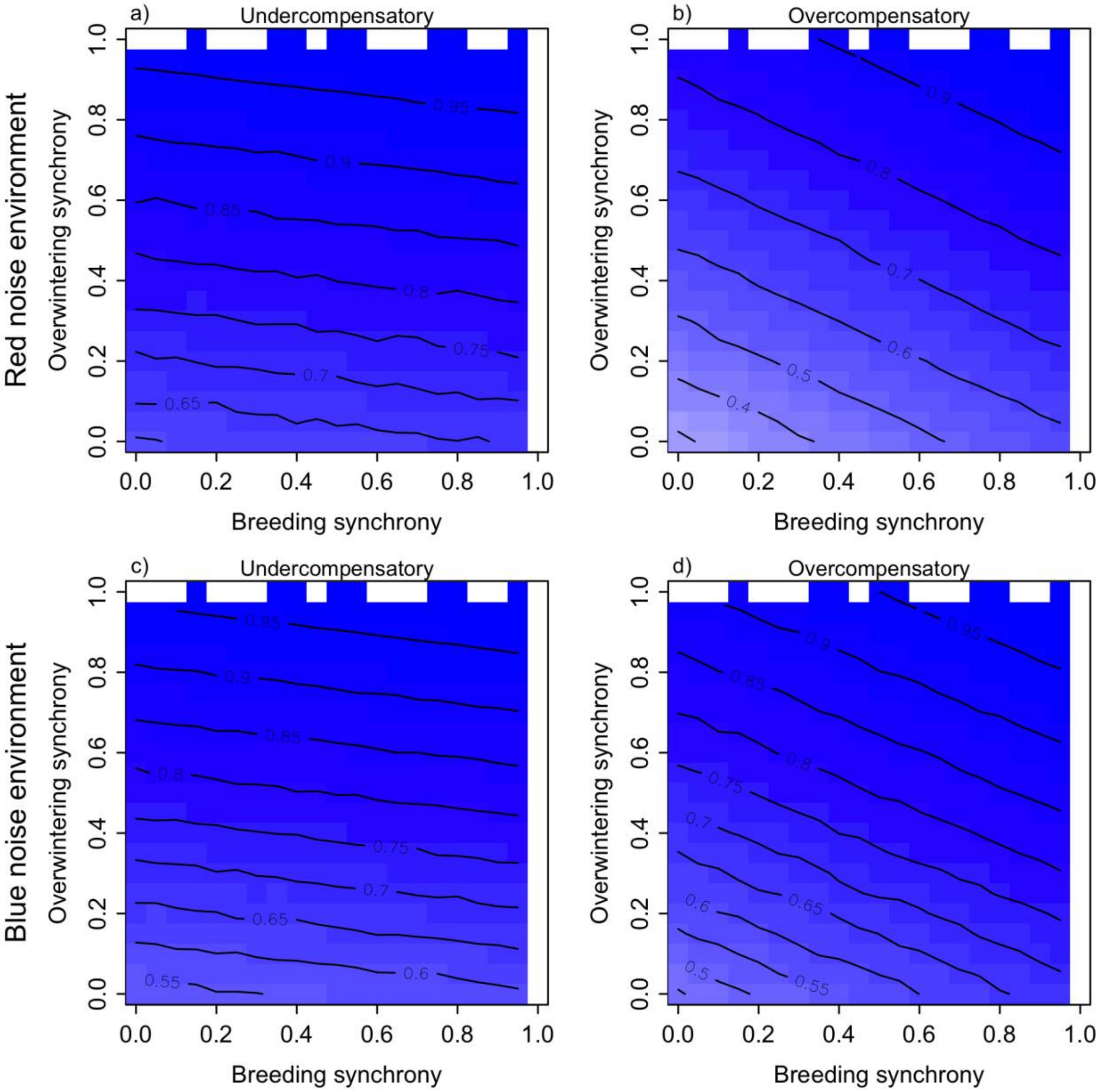

Figure S.11: Population synchrony ($cor(N_i(t), N_j(t))$) when the environmental drivers exhibit interannual correlation. The "red noise" environments have positive lag-1 autocorrelation (0.5) and the "blue noise" environments have negative lag-1 autocorrelation (-0.5). Parameter values are as in main text Figure 5 otherwise. Missing data corresponds to edge case parameter combinations for which the environmental driver covariance matrix was not positive-definite, causing technical challenges with generating driver time series.